Check for updates

Choo Le Qin (Orcid ID: 0000-0001-8383-2926)
Goetze Erica (Orcid ID: 0000-0002-7273-4359)

Genome-wide phylogeography reveals cryptic speciation in the circumglobal planktonic calcifier *Limacina bulimoides*

L.Q. Choo[1,2,3], G. Spagliardi[1], M. Malinsky[4], M. Choquet[3], E. Goetze[5], G. Hoarau[3], K.T.C.A. Peijnenburg[1,2]

[1]*Plankton Diversity and Evolution, Naturalis Biodiversity Center, Leiden, 2300 RA, the Netherlands*

[2]*Department of Freshwater and Marine Ecology, Institute for Biodiversity and Ecosystem Dynamics, University of Amsterdam, Amsterdam, 1090 GE, the Netherlands*

[3]*Faculty of Biosciences and Aquaculture, Nord University, 8049 Bodø, Norway*

[4]*Institute of Ecology and Evolution, University of Bern, Bern, Switzerland*

[5]*Department of Oceanography, University of Hawai'i at Mānoa, Honolulu, USA*

Correspondence to L.Q. Choo: leqin.choo@naturalis.nl , +447492654280

This article has been accepted for publication and undergone full peer review but has not been through the copyediting, typesetting, pagination and proofreading process which may lead to differences between this version and the Version of Record. Please cite this article as doi: 10.1111/mec.16931

This article is protected by copyright. All rights reserved.

Accepted Article

source: https://doi.org/10.48350/180465 | downloaded: 10.4.2024

1365294x, ja, Downloaded from https://onlinelibrary.wiley.com/doi/10.1111/mec.16931 by Universitaet Bern, Wiley Online Library on [22/03/2023]. See the Terms and Conditions (https://onlinelibrary.wiley.com/terms-and-conditions) on Wiley Online Library for rules of use; OA articles are governed by the applicable Creative Commons License

Accepted Article

Abstract

Little is known about when and how planktonic species arise and persist in the open ocean without apparent dispersal barriers. Pteropods are planktonic snails with thin shells susceptible to dissolution that are used as bio-indicators of ocean acidification. However, distinct evolutionary units respond to acidification differently and defining species boundaries is therefore crucial for predicting the impact of changing ocean conditions. In this global population genomic study of the shelled pteropod *Limacina bulimoides*, we combined genetic (759,000 single nucleotide polymorphisms) and morphometric data from 161 individuals, revealing three major genetic lineages (F_{ST} = 0.29 to 0.41): an 'Atlantic lineage' sampled across the Atlantic, an 'Indo-Pacific lineage' sampled in the North Pacific and Indian Ocean, and a 'Pacific lineage' sampled in the North and South Pacific. A time-calibrated phylogeny suggests that the lineages diverged about one million years ago, with estimated effective population size remaining high (~10 million) throughout Pleistocene glacial cycles. We do not observe any signatures of recent hybridisation, even in areas of sympatry in the North Pacific. While the lineages are reproductively isolated, they are morphologically cryptic, with overlapping shell shape and shell colour distributions. Despite showing that the circumglobal *L. bulimoides* consists of multiple species with smaller ranges than initially thought, we found that these pteropods still possess high levels of genetic variability. Our study adds to the growing evidence that speciation is often overlooked in the open ocean, and suggests the presence of distinct biological species within many other currently defined circumglobal planktonic species.

Keywords: marine zooplankton, population genomics, phylogeography, genome-wide SNPs

Introduction

1365294x, ja, Downloaded from https://onlinelibrary.wiley.com/doi/10.1111/mec.16931 by Universitaet Bern, Wiley Online Library on [22/03/2023]. See the Terms and Conditions (https://onlinelibrary.wiley.com/terms-and-conditions) on Wiley Online Library for rules of use; OA articles are governed by the applicable Creative Commons License

Accepted Article

We still know little about how species arise and persist in the open ocean, a seemingly interconnected habitat with few apparent barriers to dispersal. Although allopatric speciation has been accepted as the dominant mode of speciation (Bowen et al., 2016; Coyne and Orr, 2004; Mayr, 1954; Norris, 2000), it has been well documented that speciation can occur in the presence of high dispersal and gene flow, including in marine systems (Bendif et al., 2019; Bierne et al., 2003; De Vargas et al., 1999; Endler, 1977; Johannesson et al., 2010; Potkamp and Fransen, 2019; Schluter, 2009). To gain insight into the mechanisms of speciation in marine habitats, it is important to understand the factors that facilitate or constrain divergence, rather than categorising case studies into allopatric, parapatric or sympatric speciation (Butlin et al., 2008; Fitzpatrick et al., 2009). While marine species have a wide variety of life history traits, dispersal potentials and extent of gene flow among populations, holoplanktonic species typically represent an extreme end of this scale with high fecundities, enormous population sizes, and huge potential for dispersal and gene flow.

Many marine zooplankton species rank among the most abundant multicellular eukaryotes in the world. With their unique life history traits, such species present an interesting system to assess the impact of large population size and high dispersal potential on speciation and divergence (Bucklin et al., 2021; Faria et al., 2021). The large effective population sizes in marine zooplankton can have varying effects on evolution depending on the relative effects of selection and stochastic demographic events (Peijnenburg and Goetze, 2013). There can be higher levels of genetic diversity for selection to act upon and more effective selection due to the reduced effects of stochastic processes like genetic drift (Barrio et al., 2016; Peijnenburg & Goetze, 2013). However, the relationship between adaptation and population size may not be straightforward (Galtier, 2016), and the reduction in genetic drift slows down the accumulation of genetic differentiation between (partially) isolated

1365294x, ja, Downloaded from https://onlinelibrary.wiley.com/doi/10.1111/mec.16931 by Universitaet Bern, Wiley Online Library on [22/03/2023]. See the Terms and Conditions (https://onlinelibrary.wiley.com/terms-and-conditions) on Wiley Online Library for rules of use; OA articles are governed by the applicable Creative Commons License

Accepted Article

populations, which might also have profound effects on species divergence e.g., under mutation-order speciation models (Mani and Clarke, 1990; Schluter, 2009).

Species with widespread geographical distributions can have slight morphological variation across their range, but this variation alone may be considered insufficient to delimit sibling species (Fleminger and Hulsemann, 1987; Knowlton, 1993). In other cases, well-characterised morphological differences are deemed to be the result of a highly variable morphospecies (e.g. Apolônio Silva De Oliveira et al., 2017). Such practices resulted in an underestimation of ecologically-relevant divergence with conventional morphology-based taxonomy in many cases (Bongaerts et al., 2021).

With the increased availability of powerful genetic tools, there has been growing evidence for cryptic species complexes in the open ocean, contrary to historical expectations that many pelagic species would have circumglobal, panmictic populations (Norris, 2000; van der Spoel and Heyman, 1983). The majority of circumglobal planktonic species examined with genetic data have been found to harbour cryptic diversity, with examples ranging from diatoms (Casteleyn et al., 2010; Whittaker and Rynearson, 2017) to copepods (Andrews et al., 2014; Cornils et al., 2017; Halbert et al., 2013; Hirai et al., 2015) and other calcifying plankton, including gastropods (Burridge et al., 2019; Wall-Palmer et al., 2018), foraminifers (Darling et al., 2004; De Vargas et al., 1999; Kucera and Darling, 2002) and coccolithophores (Filatov et al., 2021; Sáez et al., 2003). Therefore, an important step for understanding the capacity of plankton to adapt to future environmental change is to assess the spatial distribution of genetic variation and potential for gene flow across their species ranges (Bell, 2013; Harvey et al., 2014; Manno et al., 2017; Munday et al., 2013; Poloczanska et al., 2016; Sunday et al., 2014). In addition, the use of an integrative taxonomy framework (Burridge et al., 2019; Padial, Miralles, De la Riva, & Vences, 2010) would be beneficial to identify any consistent morphological differences between these lineages and

1365294x, ja, Downloaded from https://onlinelibrary.wiley.com/doi/10.1111/mec.16931 by Universitaet Bern, Wiley Online Library on [22/03/2023]. See the Terms and Conditions (https://onlinelibrary.wiley.com/terms-and-conditions) on Wiley Online Library for rules of use; OA articles are governed by the applicable Creative Commons License

support the current genetic findings (McManus and Katz, 2009). Also, within pteropods, the traditional use of shell shape to classify and identify species (Bé and Gilmer, 1977; Lalli and Gilmer, 1989; van der Spoel et al., 1997), while advantageous due to the traceable morphology of shells preserved in fossils (Janssen and Peijnenburg, 2017), has been shown to be inadequate on its own, following the identification of genetically distinct cryptic species within several described morphospecies (Hunt et al., 2010; Jennings et al., 2010). More recent case studies in pteropods have also successfully combined genetic data from barcoding genes with geometric morphometrics of the shell shape to assess species boundaries (e.g., Burridge et al., 2015a, 2019; Choo et al., 2021; Shimizu et al., 2021).

Pteropods play important ecological and biogeochemical roles globally (Buitenhuis et al., 2019; Fabry et al., 2009; Hunt et al., 2008; Manno et al., 2010; Sulpis et al., 2021) and are commonly used as bioindicators for the effects of ocean acidification on marine calcifiers (Bednaršek, Harvey, Kaplan, Feely, & Možina, 2016; Fabry, McClintock, Mathis, & Grebmeier, 2009; Manno et al., 2017). However, little is known about their adaptive potential for future environmental changes, including their levels of genetic diversity and functional genomic variation. Pteropods possess thin aragonitic shells that are vulnerable to dissolution and more difficult to produce in acidified waters, which are predicted for the future (Busch et al., 2014; Mekkes et al., 2021b) and also observed along contemporary gradients of ocean acidification (Bednaršek et al., 2018; Manno et al., 2018; Mekkes et al., 2021a; Niemi et al., 2021). Shelled pteropods feed on phytoplankton and particulate matter, including bacteria and small protists, by trapping them in external mucous webs and ingesting the webs (Conley, Lombard, & Sutherland, 2018; Hunt et al., 2008; Lalli & Gilmer, 1989). Shelled pteropods also constitute a significant part of the diet of their unshelled relatives (gymnosomes), salmon and other predators from higher trophic levels in the pelagic food web (Groot & Margolis, 1991; Hunt et al., 2008; Lalli & Gilmer, 1989). Like other shelled

Accepted Article

1365294x, ja, Downloaded from https://onlinelibrary.wiley.com/doi/10.1111/mec.16931 by Universitaet Bern, Wiley Online Library on [22/03/2023]. See the Terms and Conditions (https://onlinelibrary.wiley.com/terms-and-conditions) on Wiley Online Library for rules of use; OA articles are governed by the applicable Creative Commons License

pteropods, species of the genus *Limacina* are protandrous hermaphrodites, developing from larvae into males first, before transitioning into females that lay free-floating egg strings from which free-swimming larvae hatch (Lalli and Wells, 1978). *Limacina bulimoides* is the most common warm water *Limacina* species worldwide, and is found in all tropical and subtropical oceans from ~45°N to ~40°S (Bé and Gilmer, 1977). They inhabit depths of up to 200m and exhibit diel vertical migration, where they are abundant in the upper 100m at night, and retreat to deeper waters during the day (Wormuth, 1981). This species is estimated to complete their life cycle in about one year (Wells, 1976).

Our prior work on *L. bulimoides* was limited to a subset of the species' range in the Atlantic ocean and used two barcoding genes (Choo et al., 2021). Here we investigate patterns and evolutionary origins of divergence across the entire species' range and with hundreds of thousands of genome-wide SNPs that derive from the target capture loci characterized in Choo et al., (2020). We also measured phenotypic differences and examined these within the geographic and genetic context of *L. bulimoides*, and explored the historical origins of speciation in the tropical and subtropical ocean. Overall, the work presented here represents the first global population genomics study of a marine zooplankton species, revealing the evolutionary history and extent of reproductive isolation among multiple independently evolving lineages that are morphologically cryptic.

Accepted Article

1365294x, ja, Downloaded from https://onlinelibrary.wiley.com/doi/10.1111/mec.16931 by Universitaet Bern, Wiley Online Library on [22/03/2023]. See the Terms and Conditions (https://onlinelibrary.wiley.com/terms-and-conditions) on Wiley Online Library for rules of use; OA articles are governed by the applicable Creative Commons License

Accepted Article

Material and Methods

Sample collection

Bulk plankton samples were collected in the Atlantic, Pacific and Indian Oceans during several cruises (Table 1). Specimens were collected using either oblique or vertical tows with ring nets or bongo nets (mesh size 200-505µm). Tows were conducted for 20 minutes to one hour, at approximate maximum depths ranging between 60 and 459 m. Samples were immediately preserved in 96% ethanol and stored at -20°C. The ethanol was replaced after 24 hours of preservation. *Limacina bulimoides* specimens were subsequently sorted in the laboratory and photographed in a standard orientation prior to destructive genetic work. Thus, the same set of individuals was used to obtain both genetic and phenotypic data (Supplementary Table 1).

1365294x, ja, Downloaded from https://onlinelibrary.wiley.com/doi/10.1111/mec.16931 by Universitaet Bern, Wiley Online Library on [22/03/2023]. See the Terms and Conditions (https://onlinelibrary.wiley.com/terms-and-conditions) on Wiley Online Library for rules of use; OA articles are governed by the applicable Creative Commons License

Table 1. Collection details of specimens of *Limacina bulimoides* from the global ocean. Number of specimens per sampling location used in target capture and geometric morphometric analyses are indicated. The collection dates are in the format DD/MM/YYYY. See also map in Figure 1A.

Cruise and Station	Latitude	Longitude	Date collected	Ocean basin	Max. depth (m)	Target capture	Morphometrics
NIC2_S1C3	21°16'N	21°01'W	31/12/2017	N. Atlantic	60	11	11
NIC8_S5C3	38°45'N	56°18' W	14/4/2018	N. Atlantic	120	11	11
AMT24_17	7°28'S	25°07'W	15/10/2014	Eq. Atlantic	266	11	11
NIC2_S9C3	5°58'N	47°50'W	13/1/2018	Eq. Atlantic	80	10	10
AMT24_22	24°27'S	25°03'W	21/10/2014	S. Atlantic	323	10	10
AMT24_23	27°46'S	25°01'W	22/10/2014	S. Atlantic	260	10	10
SN105_08	4°23'E	67°00'E	10/12/2015	Indian	67	11	10
KOK1703_03	22°39'N	157°41'W	3/7/2017	N. Pacific	200	10	10
KH1110_02	23°00'N	160°00'E	7/12/2011	N. Pacific	370	11	11
KH1110_05	23°00'N	179°59'E	14/12/2011	N. Pacific	n.a.	11	11
KH1110_08	22°47'N	158°06'W	19/12/2011	N. Pacific	411	11	10
KH1110_15	23°00'S	119°15'W	8/1/2012	S. Pacific	396	11	11
KH1110_18	29°59'S	107°00'W	13/1/2012	S. Pacific	459	11	11
KH1110_21	23°00'S	100°00'W	18/1/2012	S. Pacific	376	11	11
SO255_143	32°52'S	179°46'W	3/4/2017	S. Pacific	87	11	11

Accepted Article

1365294x, ja, Downloaded from https://onlinelibrary.wiley.com/doi/10.1111/mec.16931 by Universitaet Bern, Wiley Online Library on [22/03/2023]. See the Terms and Conditions (https://onlinelibrary.wiley.com/terms-and-conditions) on Wiley Online Library for rules of use; OA articles are governed by the applicable Creative Commons License

Total	161	159

Library preparation and sequencing

Specimens were prepared for sequencing as described in Choo et al., (2020). Briefly, genomic DNA was extracted from each individual with either the E.Z.N.A mollusc or insect DNA extraction kit (Omega Bio-Tek). The DNA was sheared by sonication to attain a peak length of 300 bp with a Covaris S220 or ME220 focused ultrasonicator. After sonication, the fragmented DNA was prepared into individual libraries using the NEXTflex Rapid Pre-Capture Combo Kit (Bioo Scientific). Individually barcoded libraries were subsequently pooled at equimolar concentrations with 26 to 27 libraries per pool. The target capture reaction was then performed on each pool using the myBaits Custom Target Capture kit (Arbor Biosciences), with a capture probe set specifically designed for *Limacina bulimoides*, as described in Choo et al. (2020). The baits target 2890 nuclear regions as well as the mitochondrial cytochrome *c* oxidase subunit I (COI) and nine other mitochondrial gene regions. To maximize the specificity of the capture reaction, the hybridisation time of the probes with the libraries was extended to three days, and the capture was performed twice, with 4 µl and 1.5 µl of probe mix, respectively (Choo et al., 2020). Captured library pools were sequenced in paired-end on the Illumina NextSeq 500 platform using three high-output v2 chips (150 cycles).

Alignment and variant calling

Raw sequences (a mean of 10,122,331 raw reads per individual; Genbank accessions: SAMN11131477-79, SAMN11131480-82, SAMN20293115-269) were de-multiplexed and then mapped with BWA mem 0.7.12 (Li, 2013) to a reduced contig set of the genomic assembly from Choo et al. (2020) (Genbank accession: SWLX00000000). The reduced genomic assembly contained only the relevant contigs; i.e., those contigs that were used for

Accepted Article

1365294x, ja, Downloaded from https://onlinelibrary.wiley.com/doi/10.1111/mec.16931 by Universitaet Bern, Wiley Online Library on [22/03/2023]. See the Terms and Conditions (https://onlinelibrary.wiley.com/terms-and-conditions) on Wiley Online Library for rules of use; OA articles are governed by the applicable Creative Commons License

the capture probe design. The resulting alignments were cleaned and filtered with SAMtools version 1.4.1 (Li et al., 2009) to retain only properly and uniquely mapped pairs (excluding SAM flag 3332 and reads with XA and SA tags; including SAM flag 3). On average, 3,961,477 reads (39.1%) per individual were then available for variant calling, 94.4% of which were mapped within the target capture regions (see Supplementary Table 1 for per-individual statistics). Duplicates were marked and removed with Picard version 2.18.5 (http://broadinstitute.github.io/picard). Variant calling was done using GATK 4.1.7.0, following the Variant Discovery Pipeline (Auwera et al., 2013; Depristo et al., 2011) with GNU parallel utility (Tange, 2011). Variants were first called per-individual using HaplotypeCaller and the resulting gVCF files were combined with CombineGVCFs. The combined gVCF file was then genotyped jointly across all samples using the GenotypeGVCFs tool of GATK. Finally, single nucleotide polymorphisms (SNPs) were extracted from the total variants using SelectVariants (-SelectType SNP). The total number of SNPs obtained for all 161 individuals was 1,790,328.

Quality filtering

SNPs were hard-filtered with VariantFiltration using QualByDepth (QD) <2.0, FisherStrand (FS) >40.0, StandOddsRatio (SOR) >3.0, MappingQuality (MQ) <40, MQRankSumTest (MQRankSum) <-5.0, MQRankSumTest (MQRankSum) >5.0, ReadPositionRankSum (ReadPosRankSum) <-4.0, INFO/DP >100000, guided by the best-practice suggestions on the GATK website, which reduced the number of SNPs only slightly to 1,629,382. The distribution of these SNPs across the different types of target capture probes included in our dataset is shown in Supplementary Table 3.

For the majority of analyses, SNPs were further filtered in BCFtools version 1.7 (Danecek et al., 2021) to retain only SNPs with Phred quality score >20 and with genotypes calls based on at least three reads present in at least 80% of the individuals. This resulted in

Accepted Article

1365294x, ja, Downloaded from https://onlinelibrary.wiley.com/doi/10.1111/mec.16931 by Universitaet Bern, Wiley Online Library on [22/03/2023]. See the Terms and Conditions (https://onlinelibrary.wiley.com/terms-and-conditions) on Wiley Online Library for rules of use; OA articles are governed by the applicable Creative Commons License

759,613 nuclear SNPs ready for further analyses. A summary of data processing steps, setting, and datasets used for each analysis in this study can be found in Supplementary Figure 1.

Population structure

For all population structure analyses, we excluded rare alleles. Specifically, SNPs with minor allele frequency (MAF) of <1% were removed. This resulted in a dataset containing 235,290 nuclear SNPs. We conducted a Principal Component Analysis (PCA) in PLINK v1.90b6.17 (Chang et al., 2015) and population clustering using the Admixture software (Alexander et al., 2009). We used the in-built cross–validation procedure in Admixture to estimate an appropriate value of K with the lowest cross-validation error among the values of K tested, between 2 and 8. Higher values of K were not tested as values of K between 3 and 8 showed an increasing trend (Supplementary Table 4). This was also supported by the admixture plots which became increasingly noisy for the higher values of K (7 and 8) (Supplementary Figure 3). For these two analyses, we used a subset of independent SNPs, with linkage pruning settings of window size of 50 genetic variants, window shift of 10 variant counts and r^2 of 0.2 in PLINK v1.90b6.17 (Chang et al., 2015), which resulted in 107,214 SNPs.

To explore population structure in finer detail, we also calculated nearest neighbour haplotype co-ancestry across all individuals with fineRADstructure v.0.3.2 (Malinsky et al., 2018). We used the hapsFromVCF function of RADpainter to convert all biallelic SNPs (96,355 nuclear SNPs; no linkage disequilibrium (LD) pruning) into an input format where SNPs from each of the 2609 contigs are assigned together into haplotypes. Because fineRADstructure is sensitive to variation in missing data proportion among individuals, we controlled for this in the following way. First, for each individual, we assessed the proportion of missing SNPs within each locus (i.e. contig). Where this proportion was more than 50%,

Accepted Article

1365294x, ja, Downloaded from https://onlinelibrary.wiley.com/doi/10.1111/mec.16931 by Universitaet Bern, Wiley Online Library on [22/03/2023]. See the Terms and Conditions (https://onlinelibrary.wiley.com/terms-and-conditions) on Wiley Online Library for rules of use; OA articles are governed by the applicable Creative Commons License

the entire locus was considered "missing" in that individual. Second, we excluded five individuals who had unusually high proportion (>4%) of such missing loci. For the remaining 156 individuals, we used the paint function of RADpainter to calculate a co-ancestry matrix, which summarises the nearest neighbour haplotype relationships in the dataset. Next, a clustering dendrogram of shared ancestry was inferred from the co-ancestry matrix using the fineSTRUCTURE Markov chain Monte Carlo clustering algorithm, with 100,000 burn-in iterations, 100,000 sample iterations, and thinning of 1000. The inferred clusters were arranged with a simple tree building algorithm in fineSTRUCTURE with 10,000 hill-climbing iterations.

For the calculation of F_{ST} we used the Weir and Cockerham (1984) estimator, implemented in VCFtools v.0.1.15 (Danecek et al., 2011) via the –weir-fst-pop option. We started from the same MAF filtered dataset as for PCA and Admixture and, to avoid bias due to genetic linkage of some loci, these estimates were obtained with thinned SNP datasets, where one SNP was randomly chosen per contig and F_{ST} was calculated for each thinning iteration, for 1000 iterations (achieved using a custom script from (Choquet et al., 2019)). The resulting distributions for each lineage and pairwise comparisons were plotted in R version 4.0.3 (R Core Team, 2017).

Genetic signals from the targeted mitochondrial COI fragments were separately analysed in a haplotype network after mapping and *de novo* assembly in Geneious Prime 2021.1.1 (https://www.geneious.com). First, all raw Illumina NextSeq reads of each of the 161 individuals were mapped to a reference database containing 355 unique *L. bulimoides* COI sequences of 564 base pairs sequenced from the Atlantic and Pacific Ocean (NCBI: MN952611-MN952965), using the Geneious assembler with medium-low sensitivity. The

Accepted Article

1365294x, ja, Downloaded from https://onlinelibrary.wiley.com/doi/10.1111/mec.16931 by Universitaet Bern, Wiley Online Library on [22/03/2023]. See the Terms and Conditions (https://onlinelibrary.wiley.com/terms-and-conditions) on Wiley Online Library for rules of use; OA articles are governed by the applicable Creative Commons License

mapped reads were extracted and *de novo* assembled per individual using the Geneious assembler with medium sensitivity. The resulting contigs were annotated for the COI region, and the COI annotation (564 bp) with the highest coverage for each individual was translated to check that there were no stop codons or frameshift mutations before being extracted. The 161 COI annotations (Genbank accessions: MZ542566 - MZ542726) were combined with one representative from each known haplogroup from (Choo et al., 2021): the Atlantic haplogroups 1 and 2, and the Pacific haplogroup (Genbank accessions: MN952611, MN952937, MN952944), and used to create a multiple sequence alignment using MAFFT v7.222 (Katoh and Standley, 2013). A minimum spanning network was calculated from the alignment and visualised in POPART (Leigh and Bryant, 2015).

Genetic diversity

To estimate genetic diversity within the major lineages, we calculated heterozygosity (average proportion of heterozygous sites in a sequence), nucleotide diversity (π) and inbreeding coefficient within the target capture probe regions for nuclear contigs. This was based on the hard-filtered SNP dataset (1,629,382 SNPs; see Supplementary Figure 1) divided into three VCFs, one for each major genetic lineage. We used the command RegionsPiGeneral from the evo toolkit (https://github.com/millanek/evo; v.0.1 r27) to perform the calculations, specifying the location of the target capture probe regions on each contig by supplying a BED-format file. We excluded results for loci where the target capture was not entirely successful, which we defined as less than 80% of the probe having <15x average coverage per individual, in line with Choo et al., (2020), and removed probes mapping to known mitochondrial contigs. For the remaining nuclear probes (2,265 probes; 78% of total) both heterozygosity and π are based on dividing the number of differences between/among sequences by the length of each probe region. Using the same set of 2,265 capture probe sequences, we also calculated per-individual estimates of the inbreeding

Accepted Article

1365294x, ja, Downloaded from https://onlinelibrary.wiley.com/doi/10.1111/mec.16931 by Universitaet Bern, Wiley Online Library on [22/03/2023]. See the Terms and Conditions (https://onlinelibrary.wiley.com/terms-and-conditions) on Wiley Online Library for rules of use; OA articles are governed by the applicable Creative Commons License

coefficient F using VCFtools 0.1.15 (Danecek et al., 2011) with the setting --het for the lineage-specific VCFs. Distributions of heterozygosity and nucleotide diversity for each genetic lineage were plotted in R version 4.0.3 (R Core Team, 2017).

Phylogenetic and demographic analyses

To infer a time-calibrated Bayesian tree, we generated a new SNP dataset, including the sister species *L. trochiformis*. SNP calling was performed with all 161 *L. bulimoides* individuals and 11 *L. trochiformis* individuals (NCBI: SAMN111131501-09, SAMN20293270, SAMN20293271from Choo et al., 2020). The *L. trochiformis* individuals were included to root the phylogeny and calibrate the age of divergence. SNP calling was followed by quality filtering using the early mentioned settings to obtain a dataset of biallelic nuclear SNPs. Since coalescent analyses do not require a large number of individuals (Felsenstein, 2006), to reduce computational effort, we randomly selected two *L. trochiformis* individuals and 10 individuals from each of the *L. bulimoides* genetic lineages to include in our analyses. SNPs corresponding to these 32 selected individuals were re-filtered to retain only biallelic nuclear SNPs. This resulting SNP dataset was thinned with VCFtools 0.1.15 (Danecek et al., 2011) to select 1 SNP every 100 bp to reduce linkage between the SNPs, resulting in a final dataset of 19,669 thinned, biallelic nuclear SNPs. Finally, we selected SNPs that were shared across all four taxa, including the outgroup, resulting in 1,279 SNPs suitable for the SNAPP analysis described below.

A SNAPP (Bryant et al., 2012) species tree was inferred in BEAST2 v2.6.2 (Bouckaert et al., 2019), using the approach demonstrated in Stange et al., (2018). We used a custom ruby script (https://github.com/mmatschiner/snapp_prep/blob/master/snapp_prep.rb), with a strict clock substitution rate calibrated with an *a priori* age constraint of divergence between *L. trochiformis* and *L. bulimoides* (Peijnenburg et al., 2020). The script was modified to allow for unlinked population sizes between the three lineages. The divergence time

Accepted Article

1365294x, ja, Downloaded from https://onlinelibrary.wiley.com/doi/10.1111/mec.16931 by Universitaet Bern, Wiley Online Library on [22/03/2023]. See the Terms and Conditions (https://onlinelibrary.wiley.com/terms-and-conditions) on Wiley Online Library for rules of use; OA articles are governed by the applicable Creative Commons License

between *L. trochiformis* and *L. bulimoides* was estimated at 13.57 Ma (95% Confidence Interval (CI) = 9.2804-20.9182 Ma), which was approximated to a lognormal distribution of (0, 13.57, 0.2), with a 95% CI of 8.99-19.7. The generation time of *L. bulimoides* was assumed to be one year (Wells, 1976) in order to calibrate the estimated effective population size. We used Tracer (Rambaut et al., 2018) to observe that all Effective Sample Size (ESS) parameters converged to stationarity with values above 200 after 1,500,000 MCMC iterations, for three independent trials. The maximum clade credibility trees with mean heights were produced in TreeAnnotator v2.6.0 (Bouckaert et al., 2014). The effective population size (N_e) and their 95% highest posterior density (HPD) confidence intervals for each of the three genetic lineages were calculated with θ from the SNAPP analysis, according to the following formula: $N_e = \theta/4\mu$, where the mutation rate μ was given as the log_clock_rate divided by $1x10^6$ with a generation time of 1 year. To assess support for the lineages as different species, we ran SNAPP together with BFD* (Leaché et al., 2014), an approach for Bayes factor delimitation, for the following models of species delimitation: all lineages being separate species, Indo-Pacific and Pacific lumped as one species, and all three lineages as one species. We ran the path-sampling for 48 steps, with chain length of 100,000 and preBurnin of 10,000. Support for the different models was assessed using marginal likelihood estimates and Bayes Factor (Kass and Raftery, 1995).

To estimate levels of gene flow between the Atlantic and other two lineages, we ran an ABBA-BABA test for all 161 individuals from the three lineages of *L. bulimoides* and 11 individuals from their sister species *L. trochiformis*, which we used as an outgroup. We used the SNP dataset that was prepared for the SNAPP analysis above, but retained all 172 individuals and did not thin the SNPs. Therefore, a total of 383,675 biallelic SNPs were used as input for the analysis in Dsuite v0.5 r44 (Malinsky and Matschiner, 2021) using the Dtrios command with the tree topology from the previously inferred SNAPP phylogeny.

Accepted Article

1365294x, ja, Downloaded from https://onlinelibrary.wiley.com/doi/10.1111/mec.16931 by Universitaet Bern, Wiley Online Library on [22/03/2023]. See the Terms and Conditions (https://onlinelibrary.wiley.com/terms-and-conditions) on Wiley Online Library for rules of use; OA articles are governed by the applicable Creative Commons License

Demographic changes for each lineage were reconstructed using Stairway Plot v2.1.1 (Liu and Fu, 2020). We used biallelic SNPs from nuclear probes that passed the coverage requirement for the genetic diversity estimates (2,265 probes; 78% of total), with a total of 1,448,243 sites (polymorphic + fixed) across these probes. Using VCFtools 0.1.15 (Danecek et al., 2011), we removed sites that showed a heterozygosity excess across all individuals (P_HET_EXCESS<0.01) as it could be indicative of bad mapping. The resulting VCF file was used to calculate the site frequency spectrum (SFS) for each lineage with easySFS (https://github.com/isaacovercast/easySFS). For each SFS, 200 subsampling iterations were conducted, as in the default recommendations. Population size estimates were truncated at 1000 years as there were insufficient samples to reconstruct demographic changes in more recent time. To put the population size estimates in context of climatic changes, we compared the timing of demographic changes with the Marine Isotope Stages derived from Lisiecki and Raymo (2005).

The mutation rate estimated by SNAPP is based only on the variable sites provided to this software and, therefore, is not meaningful outside of the SNAPP analysis. To obtain a mutation rate estimate suitable for use in the Stairway Plot analysis above, we used the same dataset with 2,265 probes, and calculated 'net sequence divergence', i.e. d_a of Cruickshank and Hahn (2014), between the lineages: Atlantic vs. Pacific ($d_a = 0.005352$), Atlantic vs. IndoPacific ($d_a = 0.007948$), and IndoPacific vs. Pacific ($d_a = 0.004463$). Dividing these values by the SNAPP-estimated divergence times between these pairs of lineages, and, as elsewhere, assuming one year per generation, we obtained the estimate $\mu = 5.22 \times 10^{-9}$.

The mode of speciation between the three lineages was inferred through testing various demographic scenarios with fastsimcoal2 (fsc27093) (Excoffier et al., 2021, 2013). We used the biallelic nuclear SNP dataset described earlier for the Stairway Plot analysis and generated a multidimensional SFS file comprising all three lineages using easySFS. With the

Accepted Article

1365294x, ja, Downloaded from https://onlinelibrary.wiley.com/doi/10.1111/mec.16931 by Universitaet Bern, Wiley Online Library on [22/03/2023]. See the Terms and Conditions (https://onlinelibrary.wiley.com/terms-and-conditions) on Wiley Online Library for rules of use; OA articles are governed by the applicable Creative Commons License

phylogeny and mean divergence times derived from the SNAPP analysis, and the previously estimated mutation rate of 5.22×10^{-9}, we evaluated the following evolutionary models: 1) no gene flow, 2) constant gene flow between all lineages, 3) recent gene flow between the Indo-Pacific and Pacific lineages, to test for a secondary contact model, and 4) ancient gene flow between the Indo-Pacific and Pacific lineages, to test for a sympatric/parapatric model of evolution. The start of gene flow was set to 100ky from the present for the recent gene flow model, and 100ky after lineages split for the parapatric model, while the amount of gene flow was allowed to vary. All gene flow was assumed to be symmetrical. Each model was run 100x to infer the most likely parameters for effective population size and amount of gene flow. We then assessed the models based on the likelihood distribution from the 100 runs, as well as the Akaike Information Criterion (AIC), which takes into account model complexity, using the script https://github.com/speciationgenomics/scripts/blob/master/calculateAIC.sh.

Shell morphology

All 161 *L. bulimoides* individuals used for genetic analyses were photographed in a standardised apertural orientation using a Zeiss V20 stacking stereomicroscope with Axiovision software prior to destructive DNA extraction. The shell images were digitised at 11 (semi-) landmarks (Supplementary Figure 2) using TpsUtil and TpsDig (Rohlf, 2015). 159 of the 161 *L. bulimoides* individuals had the complete set of landmarks and could be included in the geometric morphometric analysis. Coordinates of the (semi-) landmarks were analysed in TpsRelW (Rohlf, 2015), using a generalised least-squares Procrustes superimposition (Rohlf & Slice, 1990; Zelditch, Swiderski, Sheets, & Fink, 2004).

A repeatability analysis was conducted with a subset of 30 individuals, comprising two individuals from each of the 15 locations. Images of these individuals were landmarked at the 11 (semi-)landmarks by two independent researchers. Centroid size and relative warp (RW) scores between the pairs of images per specimen after Procrustes Fit were compared

Accepted Article

1365294x, ja, Downloaded from https://onlinelibrary.wiley.com/doi/10.1111/mec.16931 by Universitaet Bern, Wiley Online Library on [22/03/2023]. See the Terms and Conditions (https://onlinelibrary.wiley.com/terms-and-conditions) on Wiley Online Library for rules of use; OA articles are governed by the applicable Creative Commons License

using intra-class coefficient (ICC) in PAST3.0 (Hammer et al., 2001), and ICC values greater than 0.75 were considered sufficiently repeatable.

We tested for significant variation in shell shape across genetic lineages with a non-parametric Permutational Multivariate Analysis of Variance (one-way PERMANOVA) using Euclidean distances and 9999 permutations with the vegan package in R (Oksanen et al., 2019). Only the six repeatable RWs were used in the one-way PERMANOVA. The first two RW axes were plotted to visualise shell shape variation for different genetic lineages of *L. bulimoides*. Additionally, a Canonical Variates Analysis (CVA) was conducted in R (R Core Team, 2017) to discriminate shell morphometric differences between genetic lineages. A one-way ANOVA with a post-hoc Tukey HSD test was also conducted in R to test if the means of the canonical variate for each genetic lineage were different from the other groups. We also examined the effect of sampling location on shell shape, by conducting the above analyses with the four ocean basins (Atlantic, Indian, N. Pacific and S. Pacific) instead of the three genetic lineages.

We also assessed shell colour variation by qualitatively scoring aperture colour as either transparent, pink, tan or red-brown. We chose to score the colour of the aperture as it was not obscured by the tissue, which could interfere with colour identification. Also, the shell was thicker at the aperture, making it easier and more reliable to observe the colour. Scoring was done by two independent researchers to ensure repeatability of the colour scores. We tested then whether aperture colour was randomly distributed across location using a Fisher's exact test of independence.

Results

Accepted Article

1365294x, ja, Downloaded from https://onlinelibrary.wiley.com/doi/10.1111/mec.16931 by Universitaet Bern, Wiley Online Library on [22/03/2023]. See the Terms and Conditions (https://onlinelibrary.wiley.com/terms-and-conditions) on Wiley Online Library for rules of use; OA articles are governed by the applicable Creative Commons License

Accepted Article

Global genetic structure

Overall, we observed three highly divergent genetic lineages that exhibited no evidence of recent admixture, namely, the Atlantic, Indo-Pacific and Pacific lineages (Figure 1). The Atlantic lineage was comprised of all 63 individuals sampled in the Atlantic basin, the Indo-Pacific lineage comprised 38 individuals sampled from the North Pacific and the Indian Ocean site, and the Pacific lineage was comprised of 60 individuals sampled from both the North and South Pacific. The Indo-Pacific and Pacific lineages were sympatric at three sites in the North Pacific where they appeared equally common; across the three sites we sampled 16 individuals representing the Indo-Pacific lineage and 16 individuals representing the Pacific lineage (Supplementary Table 2). The Principal Component Analysis (PCA) plot revealed three genetic clusters with no intermediates between them (Figure 1B). The first two Principal Component (PC) axes comprised 39.7% of the total genetic variation; PC1 (23%) shows the Atlantic as a clearly distinct lineage, whereas PC2 (16.7%) separates all three lineages. Congruently, three genetic clusters were the best supported by the Admixture analysis (Figure 1C), as K=3 gave the lowest cross-validation error of 0.232.

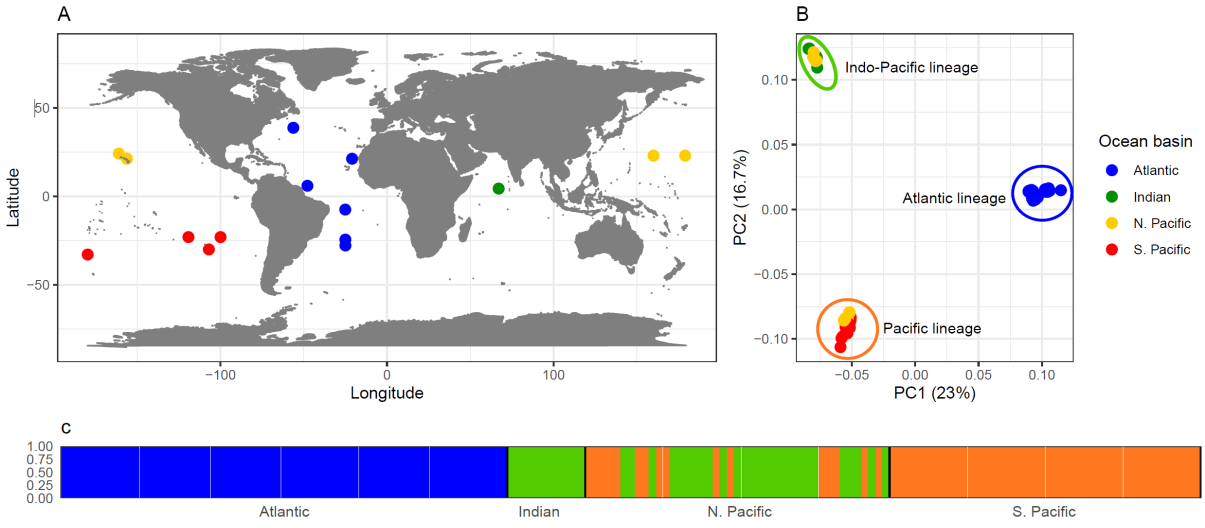

Figure 1. A) Geographic locations of the 15 sampling sites for *Limacina bulimoides*, coloured according to ocean basin: Atlantic, Indian, North (N.) and South (S.) Pacific Ocean (see legend). B) Principal Component Analysis (PCA) plot based on 107,214 nuclear SNPs from 161 individuals, illustrating the global genetic structure within this species. The three main genetic lineages are indicated with coloured circles: Atlantic (blue), Indo-Pacific (green), Pacific (orange). C) An

1365294x, ja, Downloaded from https://onlinelibrary.wiley.com/doi/10.1111/mec.16931 by Universitaet Bern, Wiley Online Library on [22/03/2023]. See the Terms and Conditions (https://onlinelibrary.wiley.com/terms-and-conditions) on Wiley Online Library for rules of use; OA articles are governed by the applicable Creative Commons License

Admixture plot showing three genetic clusters (K=3, which had the lowest cross-validation error). Each line represents one individual, while colour represents admixture proportion corresponding to each genetic cluster (Atlantic lineage in blue, Indo-Pacific lineage in green, and Pacific lineage in orange). The fine white lines represent boundaries between the different sampling stations, while the thick black lines represent the different ocean basins.

The same three genetic clusters were also recovered from the nearest neighbour haplotype co-ancestry matrix generated by fineRADstructure (Figure 2). In addition, we saw that the Atlantic lineage is comprised of three sub-clusters corresponding geographically to North, Equatorial and South Atlantic sampling sites (Table 1), consistent with previous findings based on barcoding genes (Choo et al., 2021). Within the Indo-Pacific and Pacific lineages, there were also smaller subsets of individuals with relatively higher shared co-ancestry consistent with geographic clustering. These sub-clusters corresponded to individuals from the Indian Ocean site within the Indo-Pacific lineage, and individuals from North Pacific sites within the Pacific lineage (Figure 2).

Accepted Article

1365294x, ja, Downloaded from https://onlinelibrary.wiley.com/doi/10.1111/mec.16931 by Universitaet Bern, Wiley Online Library on [22/03/2023]. See the Terms and Conditions (https://onlinelibrary.wiley.com/terms-and-conditions) on Wiley Online Library for rules of use; OA articles are governed by the applicable Creative Commons License

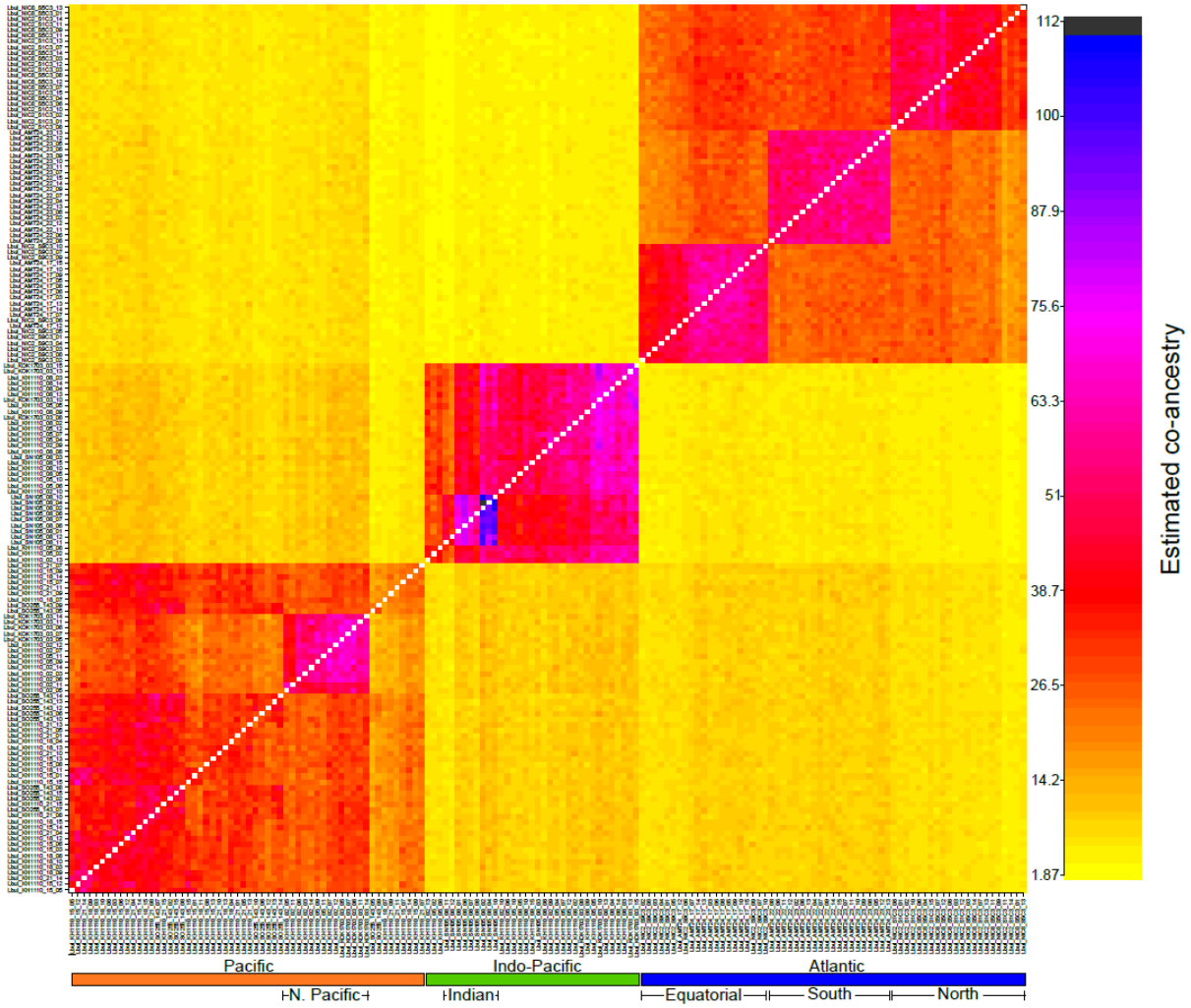

Figure 2. Co-ancestry matrix for 156 individuals, coloured according to the number of loci (contigs) at which two individuals are each other's closest relatives (see legend: black/blue colours indicate more relatedness while yellow indicates less relatedness). The three main genetic lineages (Atlantic, Indo-Pacific and Pacific) can be identified, along with finer scale structure within each lineage. The Atlantic lineage (blue) can be further sub-divided into three geographic regions with higher co-ancestry: North, Equatorial and South Atlantic. Within the Indo-Pacific lineage (green), there is higher co-ancestry within the Indian Ocean locality compared to the North Pacific sampling sites. Within the Pacific lineage (orange), the North Pacific individuals have a higher co-ancestry than with the South Pacific lineages.

Pairwise F_{ST} comparisons indicate substantial allele frequency divergence among the major lineages. Interestingly, mean F_{ST} was highest between the Atlantic and Indo-Pacific lineages (F_{ST} = 0.410), while the mean F_{ST} values between Indo-Pacific and Pacific lineages (F_{ST} = 0.300), and the Atlantic and Pacific lineages (F_{ST} = 0.293) were similar (Figure 3A).

Accepted Article

1365294x, ja, Downloaded from https://onlinelibrary.wiley.com/doi/10.1111/mec.16931 by Universitaet Bern, Wiley Online Library on [22/03/2023]. See the Terms and Conditions (https://onlinelibrary.wiley.com/terms-and-conditions) on Wiley Online Library for rules of use; OA articles are governed by the applicable Creative Commons License

Consistent with the fineRADstructure results, within-lineage mean F_{ST} values also indicate genetic substructure within all major lineages, the most within the Atlantic lineage (F_{ST} = 0.127), but also within the Indo-Pacific (F_{ST} = 0.0321) and Pacific (F_{ST} = 0.0429) (Figure 3A). All three within-lineage F_{ST} values were significantly higher than zero ($p < 2.2e-16$, one tailed t-test). We also calculated the inbreeding coefficient F_{IS} for each individual, which was on average slightly positive in all lineages: 7.8% in Atlantic ($p < 2.2e-16$; one-tailed t-test), 2.9% in Pacific ($p = 0.005$), and 1.5% Indo-Pacific ($p = 0.12$). These slightly positive F_{IS} values are consistent with the within-lineage sub-structuring reported above. At the same time, the fact that the F_{IS} values are only slightly positive indicates that outcrossing appears to be the rule in natural populations, despite *L. bulimoides* being hermaphrodites.

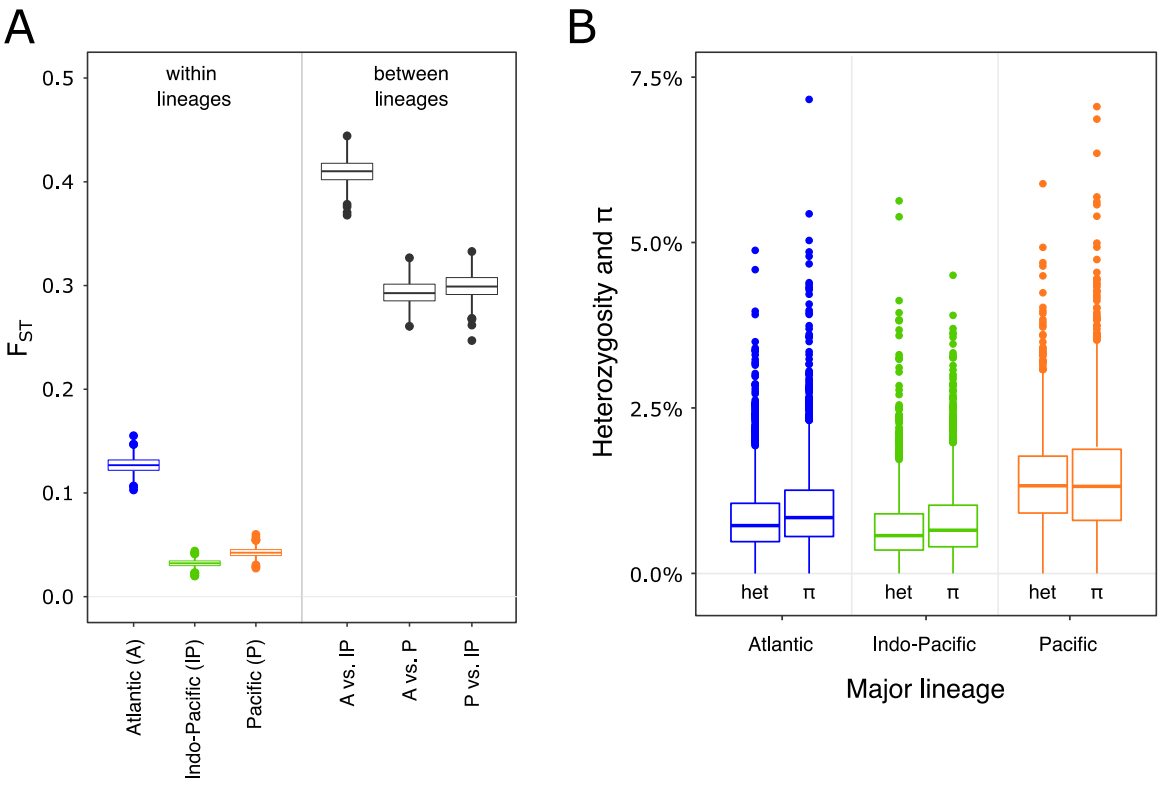

Figure 3. Characterising genetic structuring and diversity of *Limacina bulimoides* based on nuclear SNPs. A) Weir and Cockerham estimates of F_{ST} within and between the major genetic lineages: Atlantic (N= 63), Indo-Pacific (N=38) and Pacific (N=60). The distribution is over 1000 random subsamples of unlinked SNPs (see Methods for details). B) Estimates of heterozygosity and nucleotide diversity (π) within each of the major lineages. Heterozygosity was estimated as the proportion of heterozygous sites averaged across individuals. Each datapoint corresponds to the estimate for one target capture region.

Accepted Article

1365294x, ja, Downloaded from https://onlinelibrary.wiley.com/doi/10.1111/mec.16931 by Universitaet Bern, Wiley Online Library on [22/03/2023]. See the Terms and Conditions (https://onlinelibrary.wiley.com/terms-and-conditions) on Wiley Online Library for rules of use; OA articles are governed by the applicable Creative Commons License

Accepted Article

The mitochondrial COI haplotype network (Supplementary Figure 4) showed that the COI sequences were unique across all individuals, with the exception of one shared sequence between two individuals from the Atlantic Ocean. Specimens of the Atlantic lineage could be distinguished readily from the Indo-Pacific and Pacific lineages, with at least 62 nucleotide substitutions. Congruent with our previous study using barcoding genes (Choo et al. 2021), specimens from the North and Equatorial Atlantic (stations NIC2_S1C3, NIC2_S9C3, NIC8_S5C3 and AMT24_17) could be separated from specimens from the South Atlantic (stations AMT24_22 and AMT24_23) by 17 nucleotide substitutions. However, there are exceptions, namely five individuals that were sampled in the South Atlantic grouped with the North and Equatorial haplotype cluster in the mitochondrial network. Interestingly, these individuals appeared on the periphery of the haplotype cluster comprising specimens from a different sampling location (Supplementary Figure 4) but grouped according to their geographic sampling location using the nuclear SNP dataset (Figure 2). This indicates that these individuals are not recent migrants or expatriates, transported across dispersal barriers in the Atlantic Ocean, but could represent examples of introgression of mitochondrial DNA. The haploid mitochondrial genome is expected to sort faster, with shorter coalescence times as compared to the nuclear genome, so this incongruence is likely to be introgression rather than incomplete lineage sorting. The Indo-Pacific and Pacific lineages could not be clearly distinguished in the mitochondrial COI network. We observe a central cluster of individuals belonging to the Pacific lineage, composed mostly of individuals sampled from the South Pacific. From this central cluster, there are different haplotype groups consisting of individuals belonging to either the Pacific or the Indo-Pacific lineage.

1365294x, ja, Downloaded from https://onlinelibrary.wiley.com/doi/10.1111/mec.16931 by Universitaet Bern, Wiley Online Library on [22/03/2023]. See the Terms and Conditions (https://onlinelibrary.wiley.com/terms-and-conditions) on Wiley Online Library for rules of use; OA articles are governed by the applicable Creative Commons License

Accepted Article

1365294x, ja, Downloaded from https://onlinelibrary.wiley.com/doi/10.1111/mec.16931 by Universitaet Bern, Wiley Online Library on [22/03/2023]. See the Terms and Conditions (https://onlinelibrary.wiley.com/terms-and-conditions) on Wiley Online Library for rules of use; OA articles are governed by the applicable Creative Commons License

Genetic diversity

To further assess the amount of within-lineage genetic diversity within our dataset, we calculated nucleotide diversity (π) and the proportion of heterozygous sites (heterozygosity) for each individual at each of the target capture loci (Figure 3B). Both of these measures were highest within the Pacific lineage, followed by the Atlantic, and with the Indo-Pacific lineage showing the lowest genetic diversity. The values of π varied from zero to 7.2% across the target capture loci and the average values of π per lineage were 0.8% in Indo-Pacific, 1.0% in Atlantic, and 1.6% in the Pacific lineage. Heterozygosity was in all cases lower than π (Figure 3B: One-tailed t-test, Atlantic: $t_{(4341.5)} = 8.54$ $p < 2.2e^{-16}$, Indo-Pacific: $t_{(4498.7)} = 5.25$, $p = 8.02e^{-08}$, Pacific: $t_{(4280.5)} = 9.62$, $p < 2.2e^{-16}$). The values of π are only slightly above average when compared with other animals (Leffler et al., 2012; Romiguier et al., 2014), which may seem surprising given the large population sizes of planktonic species, including *L. bulimoides*. However, it is worth keeping in mind that our target capture data consist of a large proportion of coding, including non-synonymous, sites (Choo et al., 2020) and are affected by purifying and background selection, which reduce genetic diversity.

Divergence-time and population size

The SNAPP tree including three *L. bulimoides* genetic lineages and the *L. trochiformis* outgroup supported a split of the ancestral *L. bulimoides* population into the Atlantic and the Pacific/Indo-Pacific lineages (Figure 4). The divergence of the Atlantic lineage and the Indo-Pacific/Pacific lineage was estimated at 1.20 million years ago (Mya) (95% Highest Posterior Density (HPD) = 0.737- 1.76 My). The Indo-Pacific and Pacific lineages split from one another with a mean age of 0.978 My (95% HPD = 0.603-1.43 My). Consistent with the estimates of genetic diversity π, the SNAPP analyses indicate that the average estimated effective population size (N_e) was the highest for the Pacific lineage ($N_e = 6.36 \times 10^6$, 95% HPD = $4.17\text{-}8.56 \times 10^6$), followed by the Atlantic lineage ($N_e = 3.02 \times 10^6$,

95% HPD = 2.12-3.86 x10^6) and was lowest for the Indo-Pacific lineage (N_e = 1.61 x10^6, 95% HPD = 1.23-2.02 x10^6). The three lineages were best supported as separate species based on the BFD analysis (BF>10), in comparison to the other models lumping all three lineages as one species, or lumping the Indo-Pacific and Pacific lineages as one species (Supplementary Table 5).

Based on the ABBA-BABA test with the topology (((Indo-Pacific, Pacific) Atlantic) *L. trochiformis*), there was tentative evidence for excess allele sharing between the Atlantic and Pacific lineages compared to the Atlantic and Indo-Pacific lineages (D-statistic = 0.0557, Z = 2.31, p-value = 0.0208) (Supplementary Figure 5 and Supplementary Table 6). Furthermore, Fastsimcoal2 analyses, based on a joint site allele frequency spectra, suggest very limited recent gene flow (m = 1.17×10^{-6}) between the sympatric Indo-Pacific and Pacific lineages, as it was the most supported model based on likelihood distributions and AIC among the four models tested (Supplementary Figure 6, Supplementary Table 7).

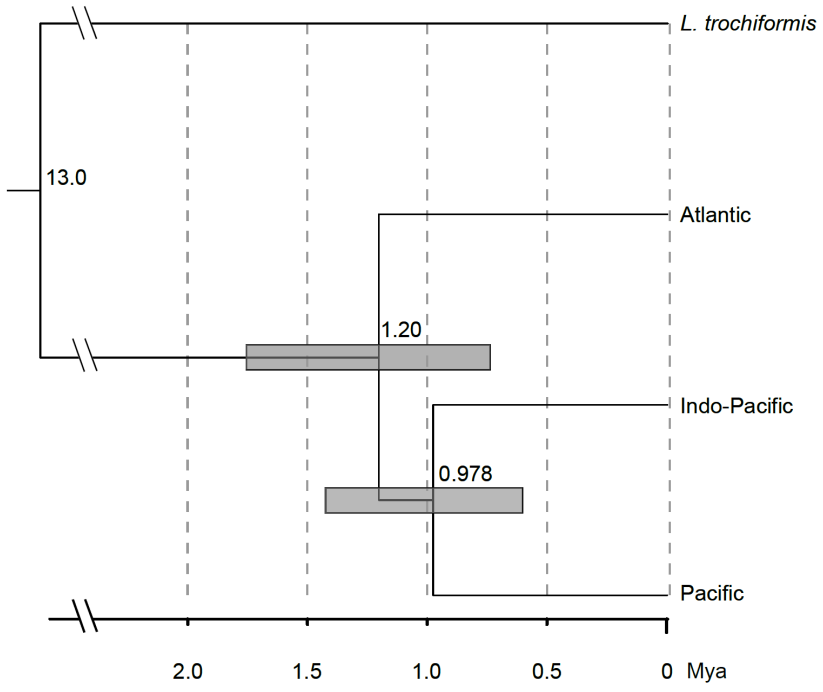

Figure 4. Maximum clade credibility tree of the SNAPP phylogeny traces divergence age of three genetic lineages of *Limacina bulimoides* to ~1 Mya. The phylogeny of the Atlantic, Indo-Pacific and

Accepted Article

1365294x, ja, Downloaded from https://onlinelibrary.wiley.com/doi/10.1111/mec.16931 by Universitaet Bern, Wiley Online Library on [22/03/2023]. See the Terms and Conditions (https://onlinelibrary.wiley.com/terms-and-conditions) on Wiley Online Library for rules of use; OA articles are governed by the applicable Creative Commons License

Pacific *L. bulimoides* and *L. trochiformis* was based on 1,279 thinned, biallelic nuclear SNPs. Two individuals of *L. trochiformis* and ten individuals per lineage of *L. bulimoides* were included in this tree. The long branches at the root were truncated to allow for better visualisation of the recent divergences. The mean age of each node is labelled above the node, and the bars indicate the 95% highest posterior densities. The scale at the bottom represents time in million years ago (Mya).

To estimate historical changes in N_e in the three major lineages, we used stairway plot analyses (Methods). The stairway plot approach indicates that all three lineages had similar demographic histories, with N_e increase followed by a long period of stable high N_e and a recent N_e decrease (Figure 5). The steep increase in N_e to ~10 million is estimated about 900 kya for the Pacific lineage, corresponding approximately to Marine Isotope Stage (MIS) 23, while similar increases were estimated to be more recent in the Atlantic (500 kya; MIS 12) and Indo-Pacific (400 kya; MIS 10). The analysis then indicates that N_e in all lineages remained stable through repeated glaciations and interglacial periods (400 kya to 15 kya; MIS 9 to MIS 2). From MIS 1 (14 kya), the start of the Holocene interglacial at 10,000 years ago, N_e across the three lineages decreased. While the timing of many of the reconstructed N_e changes corresponding to MIS transitions is intriguing, we note that purifying and background selection in our dataset is likely to have a considerable impact on the N_e estimates presented above, and could especially explain the recent N_e decrease. It will therefore be very interesting to see if similar demographic patterns are recovered in future studies using neutral markers. In addition, the evolutionary scenarios tested support the large effective population sizes (at least four million) of the three present-day, and ancestral populations, which correspond with our results in the SNAPP and Stairway plot analyses, and rule out population bottlenecks.

Accepted Article

1365294x, ja, Downloaded from https://onlinelibrary.wiley.com/doi/10.1111/mec.16931 by Universitaet Bern, Wiley Online Library on [22/03/2023]. See the Terms and Conditions (https://onlinelibrary.wiley.com/terms-and-conditions) on Wiley Online Library for rules of use; OA articles are governed by the applicable Creative Commons License

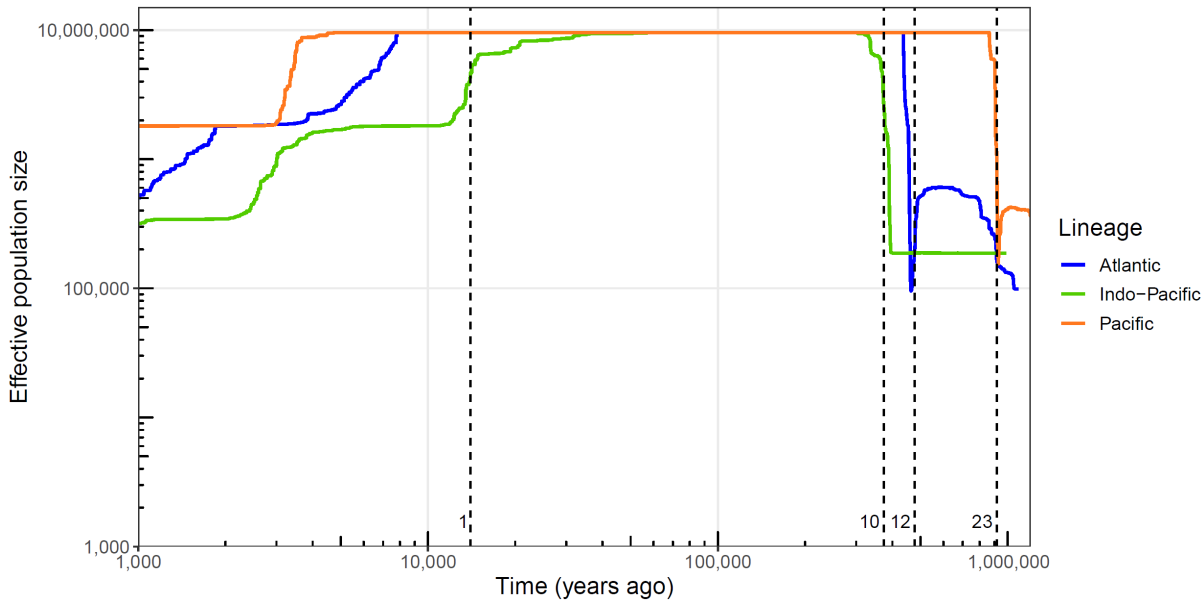

Figure 5. Effective population size (N_e) of the three *Limacina bulimoides* lineages through time as reconstructed by a stairway plot. The x-axis is the number of years before present, assuming a generation time of one year. Estimates of median N_e are coloured per lineage. Axes are log-scaled for clearer visualisation of recent histories. Plot was truncated from 0 to 1000 years ago as sample sizes are not sufficient for reconstructing very recent events as in (Liu and Fu, 2020). Dotted lines indicate the temporal boundaries between Marine Isotope Stages corresponding to timing of the reconstructed N_e changes. Odd MIS numbers refer to interglacial stages, while even numbers refer to glacial stages, with MIS1 marking the start of the Holocene and MIS12 being one of the strongest glacials of the Quaternary period.

Morphological variation

Based on the repeatability analysis with 30 individuals landmarked independently by two observers, the relative warps (RWs) 1, 2, 3, 5, 10 and 11 were selected as repeatable parameters to be used in the geometric morphometric analyses of shell shape. Of the 161 *L. bulimoides* individuals, 159 individuals had the complete set of 11 (semi-)landmarks and were included in the analysis. The six repeatable RWs explained 83.75% of shell shape variation (Supplementary Table 8). Most of the geometric morphometric variation was due to changes in shell width as shown in RW1 accounting for 51.05% of the total variation, and relative size of the aperture as shown in RW2 explaining 18.16% of the total variation (Figure 6A). Though the shells shapes of the three genetic lineages overlapped to a large extent, the

Accepted Article

1365294x, ja, Downloaded from https://onlinelibrary.wiley.com/doi/10.1111/mec.16931 by Universitaet Bern, Wiley Online Library on [22/03/2023]. See the Terms and Conditions (https://onlinelibrary.wiley.com/terms-and-conditions) on Wiley Online Library for rules of use; OA articles are governed by the applicable Creative Commons License

distributions were significantly different (PERMANOVA: $F_{(2,156)} = 18.99$, $R^2 = 0.196$, p = 1e-04), Table 2). Likewise, shell shape was significantly different between the three genetic lineages in a canonical variate analysis (One-way ANOVA: $F_{(2,156)} = 41.16$, p = 4.42e-15) (Supplementary Figure 7, Table 2). Grouping specimens according to their sampling location also resulted in significant differences in shell shape (Supplementary Figure 8 and 9), but this is to be expected because genetic lineages are not randomly distributed in space.

Table 2. Pairwise PERMANOVA and Tukey HSD of canonical variate results for comparisons of shell shape variation between genetic lineages of *Limacina bulimoides* (Atlantic, Indo-Pacific and Pacific). All pairwise comparisons are significant, after strict Bonferroni corrections (α=0.05, p<0.0167). Significant p-values are indicated in bold.

	PERMANOVA				Tukey HSD			
Pairwise comparison	**df**	**F-value**	**R^2**	**p-value**	**Difference**	**Lower**	**Upper**	**p-value**
Atlantic - Indo-Pacific	(1,97)	13.1	0.119	**6.00e-04**	1.35	0.647	2.05	**3.11e-06**
Atlantic - Pacific	(1,121)	6.49	0.0509	**0.0139**	2.30	1.70	2.91	**0**
Indo-Pacific - Pacific	(1,94)	59.6	0.388	**1.00e-04**	0.959	0.253	1.66	**4.48e-04**

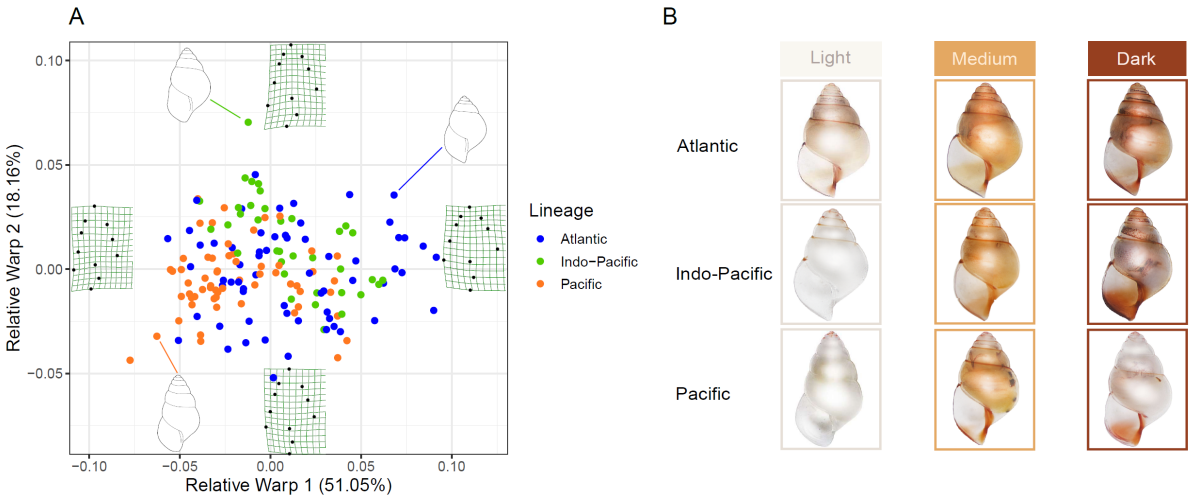

Figure 6. Variation in shell shape and aperture colour across the three lineages of *Limacina bulimoides*. A) Shell shape variation of 159 *L. bulimoides* specimens, categorised into the three genetic lineages (Atlantic, Indo-Pacific and Pacific). Shell shape variation is visualised with relative warp axes 1 and 2, explaining 51.05% and 18.16% of total shell shape variation, respectively.

Accepted Article

1365294x, ja, Downloaded from https://onlinelibrary.wiley.com/doi/10.1111/mec.16931 by Universitaet Bern, Wiley Online Library on [22/03/2023]. See the Terms and Conditions (https://onlinelibrary.wiley.com/terms-and-conditions) on Wiley Online Library for rules of use; OA articles are governed by the applicable Creative Commons License

Extremes of both relative warp axes are shown with the thin plate spline images, with each black dot corresponding to a shell landmark. Line drawings of example individuals from each genetic lineage are shown: Atlantic (Lbul_NIC2_S9C3_04), Indo-Pacific (Lbul_SN105_08_02), and Pacific (Lbul_KH1110_18_03). B) Illustration of the intensity of aperture colour observed, arranged from light, medium to dark apertures in each of the three lineages (see also Supplementary Figure 10).

We observed large variability in shell colour within our samples. The *L. bulimoides* specimens ranged in colour from almost completely white to beige to reddish-brown (Figure 6B, Supplementary Figure 10). In most coloured individuals, pale beige or red pigmentation was found on the inner aperture, lower half of the aperture, and sometimes on the sutures of the shell. Tissue pigmentation also varied widely, with dark grey tissue that is visible through the somewhat transparent shell observed in specimens from the North Atlantic and Indian Ocean, while almost completely white tissue (and shell) was mostly recorded from the South Pacific (Supplementary Figure 10). Since the colours of the shell and tissue are confounded with each other and difficult to distinguish, we limited the statistical analyses to shell aperture colour, which is not affected by tissue pigmentation.

Aperture colour was not randomly distributed with respect to genetic lineage ($p = 0.0005$, two-sided), nor sampling location ($p = 0.0005$, two-sided) (Supplementary Figure 10, Supplementary Table 10,11). Atlantic specimens had mainly pink and red-brown apertures while North Pacific specimens were highly pigmented with mainly tan and red-brown apertures. Specimens from the South Pacific had less pigmented apertures, with either transparent or pink apertures, and Indian Ocean specimens had highly pigmented shells with red-brown apertures. Aperture colour was often consistent within sampling station (six of the 15 stations) but could also vary (e.g. KH1110_05 from the North Pacific had all four aperture colours represented (Supplementary Table 9).

Accepted Article

1365294x, ja, Downloaded from https://onlinelibrary.wiley.com/doi/10.1111/mec.16931 by Universitaet Bern, Wiley Online Library on [22/03/2023]. See the Terms and Conditions (https://onlinelibrary.wiley.com/terms-and-conditions) on Wiley Online Library for rules of use; OA articles are governed by the applicable Creative Commons License

Accepted Article

Lineages in North Pacific appear morphologically cryptic

We closely examined morphological variation in individuals from the two lineages that co-occur in the North Pacific, namely the Indo-Pacific lineage (n = 16) and Pacific lineage (n = 16) (Figure 7). We found that there were no significant differences in shell shape between the two lineages despite their distinct genetic backgrounds (Figure 7B; PERMANOVA: $F_{(1,30)} = 3.75$, $R^2 = 0.111$, $p = 0.0612$). However, 81% of Pacific lineage individuals (13 out of 16) had dark pigmented spots on their tissue, which was visible through their transparent shell and none of the Indo-Pacific lineage individuals had such spots (Figure 7C). Spots were not observed on the photographs of three Pacific individuals, but these spots could have been on the opposite side that was not photographed. Dissection of additional individuals from the same samples showed that these pigmented spots were localised on the margin of their 'wing-feet' or parapodia (Supplementary Figure 11). Interestingly, these pigmented spots were not observed in the photographs of other individuals belonging to the Pacific lineage but sampled in a different location, in the South Pacific (Supplementary Figure 10).

1365294x, ja, Downloaded from https://onlinelibrary.wiley.com/doi/10.1111/mec.16931 by Universitaet Bern, Wiley Online Library on [22/03/2023]. See the Terms and Conditions (https://onlinelibrary.wiley.com/terms-and-conditions) on Wiley Online Library for rules of use; OA articles are governed by the applicable Creative Commons License

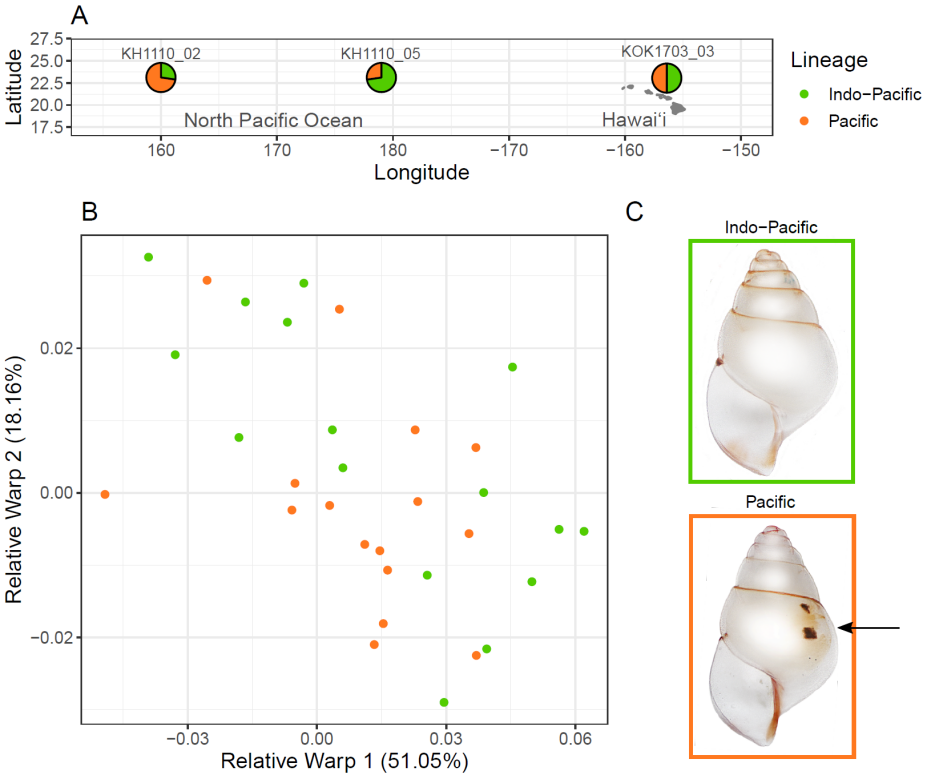

Figure 7. Distribution (A) and morphological variation (B,C) of the sympatric genetic lineages of *Limacina bulimoides* in the North Pacific with 16 individuals from the Indo-Pacific lineage (green) and 16 individuals from the Pacific lineage (orange). B) Shell shape variation as visualised with relative warps 1 and 2, which explain 51.05% and 18.16% of total shell shape variation, respectively. C) Photographs of an example individual from each genetic lineage are shown, with dark pigmented spots on the tissue, visible through the transparent shell, of the specimen from the Pacific lineage (see also Supplementary Figure 10 and 11).

Discussion

We found that the shelled pteropod *Limacina bulimoides* is composed of three main genetic lineages (Atlantic, Indo-Pacific and Pacific), the latter two of which were found in sympatry at three sampling sites in the North Pacific. We did not find any evidence for recent hybrids despite surveying genome-wide genetic variation. The evidence of very limited gene flow between the sympatric Indo-Pacific and Pacific lineages ($m = 1.17 \times 10^{-6}$) is indicative of the presence of strong isolating barriers characteristic of virtually completed speciation. Thus, these lineages remain distinct and can be considered as separate species. The Atlantic and (Indo-)Pacific lineages are allopatric, with similar levels of divergence as found for the

Accepted Article

1365294x, ja, Downloaded from https://onlinelibrary.wiley.com/doi/10.1111/mec.16931 by Universitaet Bern, Wiley Online Library on [22/03/2023]. See the Terms and Conditions (https://onlinelibrary.wiley.com/terms-and-conditions) on Wiley Online Library for rules of use; OA articles are governed by the applicable Creative Commons License

sympatric lineages, and are also likely to be reproductively isolated. The three lineages diverged approximately one million years ago (Mya) during the mid-Pleistocene, and show substantial allele frequency divergence with F_{ST} up to 40% between them. We also observed further genetic sub-structuring within each of the three lineages, consistent with geography. Morphological (shell shape) measurements revealed significant differences among the major lineages. However, unlike genetic data, which show three clear tight clusters, morphological data have overlapping distributions. Interestingly, the biological species pair in the North Pacific do not show any shell shape differences at the sampling locations where they are in sympatry, although we found dark pigmentation spots that were confined to the Pacific lineage at those stations.

We discuss possible mechanisms of reproductive isolation that are involved in maintaining the integrity of the sympatric lineages, including: a) prezygotic, such as habitat, temporal, and behavioural isolation, or b) postzygotic, such as gamete isolation and non-viability of hybrids. Specimens from three stations in the North Pacific (KH110_02, KH1110_05, and KOK1703_03) were collected by oblique tows in surface waters (maximum depth was 370 meters); therefore, it is unclear if the two lineages may have distinct depth habitats and/or corresponding diet preferences, and thus could experience habitat or ecological isolation. *Limacina bulimoides* has internal fertilisation and it is likely that they have evolved species-specific mate recognition mechanisms in order to locate each other in the pelagic environment. While they are cryptic in terms of their shell shape, the two sympatric lineages in the North Pacific could potentially be differentiated by the presence of tissue pigmentation on their parapodia (Supplementary Figure 11), reminiscent of 'pseudocryptic' species where distinguishing morphological traits are identified after initial genetic identification (Knowlton, 1993; Sáez et al., 2003). These 'wing' spots seem analogous to wing pigmentation found in butterflies and flies, which could be a convergent

Accepted Article

1365294x, ja, Downloaded from https://onlinelibrary.wiley.com/doi/10.1111/mec.16931 by Universitaet Bern, Wiley Online Library on [22/03/2023]. See the Terms and Conditions (https://onlinelibrary.wiley.com/terms-and-conditions) on Wiley Online Library for rules of use; OA articles are governed by the applicable Creative Commons License

distinguishing trait that mediates species recognition (Gompel et al., 2005; Wiernasz and Kingsolver, 1992). However, it is not known whether *Limacina*, although they are commonly referred to as 'sea-butterflies', can actually perceive such spots. *Limacina* possess eyes and optic nerves (Laibl et al., 2019), and are capable of detecting changes in light levels to trigger daily vertical migration (Cohen and Forward Jr, 2016), but there is a lack of information on the types of cues used by pteropods to recognise conspecifics. In other planktonic species, such as copepods, pheromone trails and swimming patterns are used for mate finding (Goetze and Kiørboe, 2008; Kiørboe, 2007), which may also serve to mediate the reproductive isolation between sibling species, as seen in other marine organisms like isopods, stomatopods and amphipods (Palumbi, 1994).

We have insufficient evidence to conclude whether the Pacific and Indo-Pacific lineages evolved in sympatry or have arrived at their present-day distribution through secondary contact. While we see that the model incorporating recent gene flow between the Indo-Pacific and Pacific lineages is better supported than the other models tested, we have insufficient information to discern whether the gene flow is still occurring or has occurred earlier in their evolutionary history. Based on the comparisons between the recent and ancient gene flow models (Supplementary Figure 6), the lower likelihood in the ancient gene flow model may be due to 1) gene flow after the initial split between the Atlantic and ancestral Indo-Pacific and Pacific lineages, 2) gene flow after the split between the Indo-Pacific and Pacific lineages, or 3) a combination of both factors. The absence of the Pacific lineage from the Indian Ocean, despite potential connectivity with the North Pacific, where both lineages are present, could be the result of, for example, incomplete sampling, niche incumbency effects (as in Weiner et al., 2014), recent extinction in the Indian Ocean, or a combination of factors. A recent extinction in the Indian Ocean has been recorded in the fossil record of another pteropod species (Wall-Palmer et al., 2014). More detailed sampling, in the Indian

Accepted Article

1365294x, ja, Downloaded from https://onlinelibrary.wiley.com/doi/10.1111/mec.16931 by Universitaet Bern, Wiley Online Library on [22/03/2023]. See the Terms and Conditions (https://onlinelibrary.wiley.com/terms-and-conditions) on Wiley Online Library for rules of use; OA articles are governed by the applicable Creative Commons License

and Pacific Oceans, will be needed to resolve the geographical boundaries and extent of overlap between the two lineages and to understand the causes behind their modern-day distributions. Sampling of *L. bulimoides* with depth-stratified collection techniques, metabarcoding of microbiome and gut contents, examination of their radulae, transcriptome sequencing and observations of their reproductive timings will be also be needed to gain more insight into the possible modes of current reproductive isolation between the two lineages.

Morphological variations congruent with genetic clines can indicate ecological selection or phenotypic plasticity, while the absence of morphological divergence between genetically distinct populations can result from recent colonisation, widespread gene flow or stabilising selection (Fišer et al., 2018; Milá et al., 2017). We observe both situations. Among the three main lineages, there are statistically significant differences in the (overlapping) distributions of shell shapes and aperture colours. These traits also vary among sampling locations within lineages (Supplementary Table 9, 10, 11). At the same time, when considering only the sampling locations where the Indo-Pacific and Pacific lineages appear in sympatry there are no statistical differences in shell shape. Shell shape is likely to have a phenotypically plastic component linked with life history and environmental conditions (Hoffman et al., 2010; Hollander et al., 2006; Mariani et al., 2012; Zieritz et al., 2010). Pteropod shell shape is an important trait that directly affects their sinking and swimming speeds, manoeuvrability, and their resulting ability to navigate the water column for food and evade predators (Karakas et al., 2020). In other molluscs, shell shape has been shown to be correlated with environment, either as genetically inherited differences or phenotypically plastic traits. For instance, in various species of intertidal snails with a 'crab' or 'wave' ecotype e.g., *Littorina* and *Nucella* (Guerra-Varela et al., 2009; Hollander and Butlin, 2010;

Accepted Article

1365294x, ja, Downloaded from https://onlinelibrary.wiley.com/doi/10.1111/mec.16931 by Universitaet Bern, Wiley Online Library on [22/03/2023]. See the Terms and Conditions (https://onlinelibrary.wiley.com/terms-and-conditions) on Wiley Online Library for rules of use; OA articles are governed by the applicable Creative Commons License

Johannesson, 2003; Rolán et al., 2004), or in *Mytilus* exhibiting shell shape plasticity as a response to environmental parameters such as temperature and food (Telesca et al., 2018).

The non-random variation in shell colour across sampling locations (Supplementary Figure 10) may be due to pigments incorporated from their diet, which is composed of phytoplankton, microbes and particulate matter trapped within their mucous web (Conley et al., 2018). *Limacina* can feed selectively by moving the cilia on their wings and mantle lining to sort and reject unwanted food particles (Lalli and Gilmer, 1989), and they can also control their vertical distribution through diel vertical migration. These differences in food choice and vertical habitat may lead to variable shell colour among individuals from the same sampling station. Production of shell colour has been suggested to be energetically costly across molluscs (Williams, 2017), but pteropods, with their unique planktonic lifestyle, may be subject to other selective trade-offs such as being transparent to remain inconspicuous to visual predators in the water column (Johnsen, 2001) or possessing red pigment for protection against UV radiation (Hansson, 2000).

The divergence of *L. bulimoides* lineages at around 1 Mya (Figure 4) and increase in Pacific lineage N_e (Figure 5), indicating population expansion, coincides with the timing of divergence in a mesopelagic copepod species (Andrews et al., 2014) and several coccolithophore speciation events (Filatov et al., 2021) during the mid-Pleistocene transition (0.6-1.2 Mya, between MIS22-24). This period was characterised by global cooling, lengthening of glacial cycles from 41k to 100k years, changing ocean circulation and productivity, and the evolution of many terrestrial and marine biota (Clark et al., 2006; Elderfield et al., 2012; Kender et al., 2016; McClymont et al., 2013). Changes in ocean circulation during the mid-Pleistocene transition could have facilitated the physical separation and subsequent divergence of the three lineages across the various ocean basins. These changes include the reduced exchange between the Indian and Atlantic Oceans via the

Accepted Article

1365294x, ja, Downloaded from https://onlinelibrary.wiley.com/doi/10.1111/mec.16931 by Universitaet Bern, Wiley Online Library on [22/03/2023]. See the Terms and Conditions (https://onlinelibrary.wiley.com/terms-and-conditions) on Wiley Online Library for rules of use; OA articles are governed by the applicable Creative Commons License

Agulhas leakage due to the northward migration of the Subtropical Front towards the Agulhas Plateau (Caley et al., 2012; Cartagena-Sierra et al., 2021), and the connection between the Pacific and Indian Ocean due to the weakening of the Indonesian Throughflow (Petrick et al., 2019). Similar geographical structuring across ocean basins for other circumglobal warm-water plankton species has been attributed to both physical (e.g., ocean currents or continental landmasses) and ecological (species-specific interactions with oceanographic gradients) barriers (e.g. Bendif et al., 2019; Burridge et al., 2019; Filatov et al., 2021; Goetze et al., 2015; Hirai et al., 2015), although it is unknown if these structured populations arose at the same time. Within the Pacific and Atlantic basins, habitat discontinuities like the mesotrophic equatorial upwelling waters, have been described as ecological dispersal barriers for subtropical copepods (Goetze, 2005; Goetze et al., 2017) and the pteropod genus *Cuvierina* (Burridge et al., 2015). Congruently, fossil evidence of coccolithophore species distributions point to the emergence of new species at equatorial latitudes (Filatov et al., 2021).

We found substantial levels of genetic variation in all lineages (e.g. π ranged from 0.8 to 1.6% per lineage), despite the fact that most of our targeted regions are coding and thus affected by purifying and background selection. These levels are comparable to those reported for two species of planktonic copepods (π ranging from 0.6 to 0.8%) based on a similar target capture approach but with more restricted geographic sampling (Choquet et al. 2019). This level of π, coupled with the stairway plot and SNAPP estimates of N_e for *L. bulimoides*, indicate an absence of any pronounced population bottlenecks across multiple Pleistocene glacial-interglacial transitions. This suggests that this species complex is likely to have been resilient to ocean changes associated with glacial cycles. In the stairway plot, the timing of the rapid rise of N_e in the Atlantic and Indo-Pacific lineage between MIS10-12 is coincident with MIS11, the warmest interglacial interval of the last 500 k years, with high

Accepted Article

1365294x, ja, Downloaded from https://onlinelibrary.wiley.com/doi/10.1111/mec.16931 by Universitaet Bern, Wiley Online Library on [22/03/2023]. See the Terms and Conditions (https://onlinelibrary.wiley.com/terms-and-conditions) on Wiley Online Library for rules of use; OA articles are governed by the applicable Creative Commons License

levels of atmospheric CO_2 (Siegenthaler et al., 2005), warm sea-surface temperatures and atypical blooms of calcareous plankton in the high latitudes (Howard, 1997; McManus et al., 2003). Stable population sizes in *L. bulimoides* were associated with the repeated glacials and interglacials from MIS2 to 9, including the Last Glacial Period (MIS2-4), even though pH levels fluctuated up to 0.2±0.1 pH between glacial and interglacial periods (Hönisch and Hemming, 2005; Sanyal et al., 1995). Stable abundances of *L. bulimoides* were also recorded within sediment cores in the Caribbean Sea, which had low variation in SST across both glacial and interglacial periods (Wall-Palmer et al., 2014). At the beginning of the Holocene, between 19-7 k years ago (boundary of MIS1/2), temperatures increased and global sea levels rose rapidly (Lambeck and Chappell, 2001), while atmospheric CO_2 increased by 30% (Hönisch et al., 2012; Monnin et al., 2001). These environmental changes have been linked with decreasing shell mass in other planktonic calcifiers like foraminifers and coccolithophores (Barker and Elderfield, 2002; Beaufort et al., 2011) and are associated with a decrease in N_e in our stairway plot reconstructions. However, caution in interpreting these correlations is warranted because our demographic inferences are affected by background selection (Ewing and Jensen, 2016), which is expected to result in a signal of recent N_e decrease. Another caveat is that the timings of divergence and demographic changes are a function of generation time, which was set to one year based on our knowledge of *L. bulimoides* biology. A more accurate estimate of generation time may affect these conclusions to some degree.

The very high levels of genetic diversity (heterozygosity and π) and large repetitive genomes of many marine zooplankton species hinder the adoption of genomic approaches in evolutionary studies of these organisms. By focussing on transcribed regions of the genome, the target capture approach has enabled us to greatly reduce these challenges and conduct a global genomic study in a marine zooplankton species. We note the usefulness of genome-

Accepted Article

1365294x, ja, Downloaded from https://onlinelibrary.wiley.com/doi/10.1111/mec.16931 by Universitaet Bern, Wiley Online Library on [22/03/2023]. See the Terms and Conditions (https://onlinelibrary.wiley.com/terms-and-conditions) on Wiley Online Library for rules of use; OA articles are governed by the applicable Creative Commons License

wide data, compared to mitochondrial DNA or barcoding genes, in detecting population structure and assessing species boundaries. Unlike a single locus (e.g., the mitochondrial COI barcoding region), whose evolutionary history represents a single genealogy or a *gene tree*, our set of hundreds of thousands of genome-wide SNPs allows us to unambiguously apportion the genetic structure within *L. bulimoides*. Evolutionary histories of individual genes (gene trees) and histories of populations or species (population/species trees) are seldom identical (e.g., Nichols, 2001). Moreover, in some studies using barcode regions, species delimitations have been made based on taxon-specific thresholds of levels of sequence divergence beyond which reproductive isolation is expected (Krug et al., 2013; Lefébure et al., 2006; Young et al., 2017). This method is highly effective for detecting new putative species in broad-scale barcoding studies without prior information; however, divergence distances do not necessarily indicate reproductive isolation or lead to further understanding of the process of speciation (Freeman and Pennell, 2021). The genome-wide dataset we present here will underpin future investigations into the nature of selection, adaptation, divergence and speciation in the open ocean. We expect that the predominance of coding loci in our data and the ability to separate synonymous and non-synonymous sites will be major assets in these future studies.

Despite the potential for global dispersal in *L. bulimoides*, we observed diversification of lineages across ocean basins that likely originated from the mid-Pleistocene transition. These lineages are probably distinct species with strong reproductive isolation among them, and have survived through periods of glacial-interglacial transitions representing a wide range of oceanographic conditions, including ocean alkalinity. There are slight differences in shell shape between the lineages, but shell shape alone cannot be used as a taxonomic character, and it is unclear whether environmental or genetic factors have a greater impact on shell morphology. Even though their effective population sizes may have decreased since the

Accepted Article

1365294x, ja, Downloaded from https://onlinelibrary.wiley.com/doi/10.1111/mec.16931 by Universitaet Bern, Wiley Online Library on [22/03/2023]. See the Terms and Conditions (https://onlinelibrary.wiley.com/terms-and-conditions) on Wiley Online Library for rules of use; OA articles are governed by the applicable Creative Commons License

start of the Holocene, the three lineages still possess high levels of standing genetic variation and nucleotide diversity, upon which selection could act to drive further adaptation in the future (Bernatchez, 2016; Bitter et al., 2019; Schluter and Conte, 2009). However, it is unclear whether pteropods and other planktonic calcifiers can cope with the rate of ongoing ocean changes, including anthropogenic carbon emission rates that are unprecedented since at least 66 million years, leading to increasing ocean acidification (Zeebe et al., 2016). While there are no visibly obvious dispersal barriers in the open ocean, we have found genome-wide evidence for speciation and divergence in *L. bulimoides*, and there is likely more diversity in planktonic species than meets the eye.

Acknowledgements

We thank L. Mekkes, A. Burridge and M. Jungbluth for assistance at sea, and all captains and crews of the ocean expeditions for their support and assistance. We thank D. Wall-Palmer for providing us Indian Ocean and South Pacific samples from the SN105 and SO255 cruises and A. Tsuda for providing the Pacific samples from the 2011/2012 R/V Hakuho-Maru KH-11-10 cruise. We warmly acknowledge M. Matschiner and E. Trucchi for their advice on data analyses, W. Renema and D. Wall-Palmer for helpful discussions regarding the manuscript, and M. Kopp for guidance in the lab. We also thank the four anonymous reviewers whose comments have improved this manuscript. This research was supported by the Netherlands Organisation for Scientific Research (NWO) Vidi grant 016.161.351 to K.T.C.A.P. The Netherlands Initiative Changing Oceans (NICO) expedition on *RV Pelagia* was also funded by NWO and the Royal Netherlands Institute for Sea Research (NIOZ). L.Q.C. was partly supported by a Nord University Internalisation Grant during the writing of this manuscript. Further fieldwork was supported by NSF grants OCE-1029478 and OCE-1338959 to E.G. The *R/V Sonne* cruise SO255 was funded by the German Federal Ministry of Education and Research (BMBF; grant 03G0255A), and the SN105

Accepted Article

1365294x, ja, Downloaded from https://onlinelibrary.wiley.com/doi/10.1111/mec.16931 by Universitaet Bern, Wiley Online Library on [22/03/2023]. See the Terms and Conditions (https://onlinelibrary.wiley.com/terms-and-conditions) on Wiley Online Library for rules of use; OA articles are governed by the applicable Creative Commons License

cruise on board the ORV Sagar Nidhi was funded by the Indian National Centre for Ocean Information Services (INCOIS), Ministry of Earth Sciences, India, as the first cruise of the second International Indian Ocean Expedition (IIOE-2). The Atlantic Meridional Transect is funded by the UK Natural Environment Research Council through its National Capability Long-term Single Centre Science Programme, Climate Linked Atlantic Sector Science (grant number NE/R015953/1). This study contributes to the international IMBeR project and is contribution number 368 of the AMT programme.

Data accessibility statement

The raw sequence data for *L. bulimoides* were archived on NCBI Genbank with following accessions: SAMN11131477-79, SAMN11131480-82 and SAMN20293115-269. The assembled COI sequences for *L. bulimoides* can be found on NCBI Genbank with the following accessions: MZ542566-MZ542726. Shell images for the specimens, the methods protocol for DNA extraction and target capture, and hard-filtered vcf files used for this study can be accessed on Mendeley Data using the doi: 10.17632/7m86twnzp2.1.

References

Alexander, D.H., Novembre, J., Lange, K., 2009. Fast model-based estimation of ancestry in unrelated individuals. Genome Res. 19, 1655–1664. https://doi.org/10.1101/gr.094052.109

Andrews, K.R., Norton, E.L., Fernandez-Silva, I., Portner, E., Goetze, E., 2014. Multilocus evidence for globally distributed cryptic species and distinct populations across ocean gyres in a mesopelagic copepod. Mol. Ecol. 23, 5462–5479. https://doi.org/10.1111/mec.12950

Apolônio Silva De Oliveira, D., Decraemer, W., Moens, T., Dos Santos, G.A.P., Derycke, S., 2017. Low genetic but high morphological variation over more than 1000 km coastline refutes omnipresence of cryptic diversity in marine nematodes. BMC Evol. Biol. 17, 71. https://doi.org/10.1186/s12862-017-0908-0

Auwera, G.A., Carneiro, M.O., Hartl, C., Poplin, R., del Angel, G., Levy-Moonshine, A., Jordan, T., Shakir, K., Roazen, D., Thibault, J., Banks, E., Garimella, K. V, Altshuler, D., Gabriel, S., DePristo, M.A., 2013. From FastQ data to high-confidence variant calls: The Genome Analysis Toolkit best practices pipeline. Curr. Protoc. Bioinforma. 43,

Accepted Article

1365294x, ja, Downloaded from https://onlinelibrary.wiley.com/doi/10.1111/mec.16931 by Universitaet Bern, Wiley Online Library on [22/03/2023]. See the Terms and Conditions (https://onlinelibrary.wiley.com/terms-and-conditions) on Wiley Online Library for rules of use; OA articles are governed by the applicable Creative Commons License

11.10.1-11.10.33. https://doi.org/10.1002/0471250953.bil110s43

Barker, S., Elderfield, H., 2002. Foraminiferal calcification response to glacial-interglacial changes in atmospheric Co2. Science 297, 833–836. https://doi.org/10.1126/science.1072815

Barrio, A.M., Lamichhaney, S., Fan, G., Rafati, N., Pettersson, M., Zhang, H., Dainat, J., Ekman, D., Höppner, M., Jern, P., Martin, M., Nystedt, B., Liu, X., Chen, W., Liang, X., Shi, C., Fu, Y., Ma, K., Zhan, X., Feng, C., Gustafson, U., Rubin, C.J., Almén, M., Blass, M., Casini, M., Folkvord, A., Laikre, L., Ryman, N., Lee, S.Y., Xu, X., Andersson, L., 2016. The genetic basis for ecological adaptation of the Atlantic herring revealed by genome sequencing. Elife 5, e12081. https://doi.org/10.7554/eLife.12081

Bé, A.W.H., Gilmer, R., 1977. A zoogeographic and taxonomic review of Euthecosomatous Pteropoda. Ocean. Micropaleontol. 1, 733–808.

Beaufort, L., Probert, I., De Garidel-Thoron, T., Bendif, E.M., Ruiz-Pino, D., Metzl, N., Goyet, C., Buchet, N., Coupel, P., Grelaud, M., Rost, B., Rickaby, R.E.M., De Vargas, C., 2011. Sensitivity of coccolithophores to carbonate chemistry and ocean acidification. Nature 476, 80–83. https://doi.org/10.1038/nature10295

Bednaršek, N., Feely, R.A., Beck, M.W., Glippa, O., Kanerva, M., Engström-Öst, J., 2018. El Niño-related thermal stress coupled with upwelling-related ocean acidification negatively impacts cellular to population-level responses in pteropods along the California current system with implications for increased bioenergetic costs. Front. Mar. Sci. 5, 486. https://doi.org/10.3389/fmars.2018.00486

Bednaršek, N., Harvey, C.J., Kaplan, I.C., Feely, R.A., Možina, J., 2016. Pteropods on the edge: Cumulative effects of ocean acidification, warming, and deoxygenation. Prog. Oceanogr. 145, 1–24. https://doi.org/10.1016/j.pocean.2016.04.002

Bell, G., 2013. Evolutionary rescue and the limits of adaptation. Philos. Trans. R. Soc. B Biol. Sci. 368, 20120080. https://doi.org/10.1098/rstb.2012.0080

Bendif, E.M., Nevado, B., Wong, E.L.Y., Hagino, K., Probert, I., Young, J.R., Rickaby, R.E.M., Filatov, D.A., 2019. Repeated species radiations in the recent evolution of the key marine phytoplankton lineage Gephyrocapsa. Nat. Commun. 10, 4234. https://doi.org/10.1038/s41467-019-12169-7

Bernatchez, L., 2016. On the maintenance of genetic variation and adaptation to environmental change: considerations from population genomics in fishes. J. Fish Biol. 89, 2519–2556. https://doi.org/10.1111/jfb.13145

Bierne, N., Bonhomme, F., David, P., 2003. Habitat preference and the marine-speciation paradox. Proc. R. Soc. B Biol. Sci. 270, 1399–1406. https://doi.org/10.1098/rspb.2003.2404

Bitter, M.C., Kapsenberg, L., Gattuso, J.P., Pfister, C.A., 2019. Standing genetic variation fuels rapid adaptation to ocean acidification. Nat. Commun. 10, 5821. https://doi.org/10.1038/s41467-019-13767-1

Bongaerts, P., Cooke, I.R., Ying, H., Wels, D., den Haan, S., Hernandez-Agreda, A., Brunner, C.A., Dove, S., Englebert, N., Eyal, G., Forêt, S., Grinblat, M., Hay, K.B., Harii, S., Hayward, D.C., Lin, Y., Mihaljević, M., Moya, A., Muir, P., Sinniger, F., Smallhorn-West, P., Torda, G., Ragan, M.A., van Oppen, M.J.H., Hoegh-Guldberg, O.,

Accepted Article

1365294x, ja, Downloaded from https://onlinelibrary.wiley.com/doi/10.1111/mec.16931 by Universitaet Bern, Wiley Online Library on [22/03/2023]. See the Terms and Conditions (https://onlinelibrary.wiley.com/terms-and-conditions) on Wiley Online Library for rules of use; OA articles are governed by the applicable Creative Commons License

Accepted Article

2021. Morphological stasis masks ecologically divergent coral species on tropical reefs. Curr. Biol. 31, 2286-2298.E8. https://doi.org/10.1016/j.cub.2021.03.028

Bouckaert, R., Heled, J., Kühnert, D., Vaughan, T., Wu, C.H., Xie, D., Suchard, M.A., Rambaut, A., Drummond, A.J., 2014. BEAST 2: A Software Platform for Bayesian Evolutionary Analysis. PLoS Comput. Biol. 10, e1003537. https://doi.org/10.1371/journal.pcbi.1003537

Bouckaert, R., Vaughan, T.G., Barido-Sottani, J., Duchêne, S., Fourment, M., Gavryushkina, A., Heled, J., Jones, G., Kühnert, D., De Maio, N., Matschiner, M., Mendes, F.K., Müller, N.F., Ogilvie, H.A., Du Plessis, L., Popinga, A., Rambaut, A., Rasmussen, D., Siveroni, I., Suchard, M.A., Wu, C.H., Xie, D., Zhang, C., Stadler, T., Drummond, A.J., 2019. BEAST 2.5: An advanced software platform for Bayesian evolutionary analysis. PLoS Comput. Biol. 15, e1006650. https://doi.org/10.1371/journal.pcbi.1006650

Bowen, B.W., Gaither, M.R., DiBattista, J.D., Iacchei, M., Andrews, K.R., Grant, W.S., Toonen, R.J., Briggs, J.C., 2016. Comparative phylogeography of the ocean planet. Proc. Natl. Acad. Sci. 113, 7962–7969. https://doi.org/10.1073/pnas.1602404113

Bryant, D., Bouckaert, R., Felsenstein, J., Rosenberg, N.A., Roychoudhury, A., 2012. Inferring species trees directly from biallelic genetic markers: Bypassing gene trees in a full coalescent analysis. Mol. Biol. Evol. 29, 1917–1932. https://doi.org/10.1093/molbev/mss086

Bucklin, A., Peijnenburg, K.T.C.A., Kosobokova, K., Machida, R.J., 2021. New insights into biodiversity, biogeography, ecology, and evolution of marine zooplankton based on molecular approaches. ICES J. Mar. Sci. 78, 3281–3287. https://doi.org/10.1093/icesjms/fsab198

Buitenhuis, E.T., Le Quéré, C., Bednaršek, N., Schiebel, R., 2019. Large contribution of pteropods to shallow $CaCO_3$ export. Global Biogeochem. Cycles 33, 458–468. https://doi.org/10.1029/2018GB006110

Burridge, A.K., Goetze, E., Raes, N., Huisman, J., Peijnenburg, K.T.C.A., 2015. Global biogeography and evolution of Cuvierina pteropods. BMC Evol. Biol. 15, 39. https://doi.org/10.1186/s12862-015-0310-8

Burridge, A.K., Van Der Hulst, R., Goetze, E., Peijnenburg, K.T.C.A., 2019. Assessing species boundaries in the open sea: an integrative taxonomic approach to the pteropod genus *Diacavolinia*. Zool. J. Linn. Soc. 187, 1016–1040. https://doi.org/10.1093/zoolinnean/zlz049

Busch, D.S., Maher, M., Thibodeau, P., McElhany, P., 2014. Shell condition and survival of Puget Sound pteropods are impaired by ocean acidification conditions. PLoS One 9, e105884. https://doi.org/10.1371/journal.pone.0105884

Butlin, R.K., Galindo, J., Grahame, J.W., 2008. Review. Sympatric, parapatric or allopatric: The most important way to classify speciation? Philos. Trans. R. Soc. B Biol. Sci. 363, 2997–3007. https://doi.org/10.1098/rstb.2008.0076

Caley, T., Giraudeau, J., Malaizé, B., Rossignol, L., Pierre, C., 2012. Agulhas leakage as a key process in the modes of Quaternary climate changes. Proc. Natl. Acad. Sci. U. S. A. 109, 6835–6839. https://doi.org/10.1073/pnas.1115545109

Cartagena-Sierra, A., Berke, M.A., Robinson, R.S., Marcks, B., Castañeda, I.S., Starr, A.,

1365294x, ja, Downloaded from https://onlinelibrary.wiley.com/doi/10.1111/mec.16931 by Universitaet Bern, Wiley Online Library on [22/03/2023]. See the Terms and Conditions (https://onlinelibrary.wiley.com/terms-and-conditions) on Wiley Online Library for rules of use; OA articles are governed by the applicable Creative Commons License

Accepted Article

Hall, I.R., Hemming, S.R., LeVay, L.J., Party, E. 361 S., 2021. Latitudinal migrations of the Subtropical Front at the Agulhas Plateau through the Mid-Pleistocene Transition. Paleoceanogr. Paleoclimatology 36, e2020PA004084. https://doi.org/10.1029/2020pa004084

Casteleyn, G., Leliaert, F., Backeljau, T., Debeer, A.E., Kotaki, Y., Rhodes, L., Lundholm, N., Sabbe, K., Vyverman, W., 2010. Limits to gene flow in a cosmopolitan marine planktonic diatom. Proc. Natl. Acad. Sci. U. S. A. 107, 12952–12957. https://doi.org/10.1073/pnas.1001380107

Chang, C.C., Chow, C.C., Tellier, L.C.A.M., Vattikuti, S., Purcell, S.M., Lee, J.J., 2015. Second-generation PLINK: rising to the challenge of larger and richer datasets. Gigascience 4, 7. https://doi.org/10.1186/s13742-015-0047-8

Choo, L.Q., Bal, T.M.P., Choquet, M., Smolina, I., Ramos-Silva, P., Marlétaz, F., Kopp, M., Hoarau, G., Peijnenburg, K.T.C.A., 2020. Novel genomic resources for shelled pteropods: A draft genome and target capture probes for *Limacina bulimoides*, tested for cross-species relevance. BMC Genomics 21, 11. https://doi.org/10.1186/s12864-019-6372-z

Choo, L.Q., Bal, T.M.P., Goetze, E., Peijnenburg, K.T.C.A., 2021. Oceanic dispersal barriers in a holoplanktonic gastropod. J. Evol. Biol. 34, 224–240. https://doi.org/10.1111/jeb.13735

Choquet, M., Smolina, I., Dhanasiri, A.K.S., Kopp, M., Jueterbock, A., Sundaram, A.Y.M., Hoarau, G., 2019. Towards population genomics in non-model species with large genomes: a case study of the marine zooplankton *Calanus finmarchicus*. R. Soc. Open Sci. 6, 1–36. https://doi.org/10.1098/RSOS.180608

Clark, P.U., Archer, D., Pollard, D., Blum, J.D., Rial, J.A., Brovkin, V., Mix, A.C., Pisias, N.G., Roy, M., 2006. The middle Pleistocene transition: characteristics, mechanisms, and implications for long-term changes in atmospheric pCO_2. Quat. Sci. Rev. 25, 3150–3184. https://doi.org/10.1016/j.quascirev.2006.07.008

Cohen, J.H., Forward Jr, R.B., 2016. Zooplankton diel vertical migration - A review of proximate control, in: Oceanography and Marine Biology. CRC Press, pp. 89–122.

Conley, K.R., Lombard, F., Sutherland, K.R., 2018. Mammoth grazers on the ocean's minuteness: a review of selective feeding using mucous meshes. Proc. R. Soc. B Biol. Sci. 285, 20180056. https://doi.org/10.1098/rspb.2018.0056

Cornils, A., Wend-Heckmann, B., Held, C., 2017. Global phylogeography of *Oithona similis* s.l. (Crustacea, Copepoda, Oithonidae) – A cosmopolitan plankton species or a complex of cryptic lineages? Mol. Phylogenet. Evol. 107, 473–485. https://doi.org/10.1016/j.ympev.2016.12.019

Coyne, J.A., Orr, H.A., 2004. Speciation. Sinauer Associates, Sunderland, MA.

Cruickshank, T.E., Hahn, M.W., 2014. Reanalysis suggests that genomic islands of speciation are due to reduced diversity, not reduced gene flow. Mol. Ecol. 23, 3133–3157. https://doi.org/10.1111/mec.12796

Danecek, P., Auton, A., Abecasis, G., Albers, C.A., Banks, E., Depristo, M.A., Handsaker, R.E., Lunter, G., Marth, G.T., Sherry, S.T., Mcvean, G., Durbin, R., 2011. The variant call format and VCFtools. Bioinformatics 27, 2156–2158.

1365294x, ja, Downloaded from https://onlinelibrary.wiley.com/doi/10.1111/mec.16931 by Universitaet Bern, Wiley Online Library on [22/03/2023]. See the Terms and Conditions (https://onlinelibrary.wiley.com/terms-and-conditions) on Wiley Online Library for rules of use; OA articles are governed by the applicable Creative Commons License

https://doi.org/10.1093/bioinformatics/btr330

Danecek, P., Bonfield, J.K., Liddle, J., Marshall, J., Ohan, V., Pollard, M.O., Whitwham, A., Keane, T., McCarthy, S.A., Davies, R.M., Li, H., 2021. Twelve years of SAMtools and BCFtools. Gigascience 10, 1–4. https://doi.org/10.1093/gigascience/giab008

Darling, K.F., Kucera, M., Pudsey, C.J., Wade, C.M., 2004. Molecular evidence links cryptic diversification in polar planktonic protists to Quaternary climate dynamics. Proc. Natl. Acad. Sci. U. S. A. 101, 7657–7662. https://doi.org/10.1073/pnas.0402401101

De Vargas, C., Norris, R., Zaninetti, L., Gibb, S.W., Pawlowski, J., 1999. Molecular evidence of cryptic speciation in planktonic foraminifers and their relation to oceanic provinces. Proc. Natl. Acad. Sci. U. S. A. 96, 2864–2868. https://doi.org/10.1073/pnas.96.6.2864

Depristo, M.A., Banks, E., Poplin, R., Garimella, K. V., Maguire, J.R., Hartl, C., Philippakis, A.A., Del Angel, G., Rivas, M.A., Hanna, M., McKenna, A., Fennell, T.J., Kernytsky, A.M., Sivachenko, A.Y., Cibulskis, K., Gabriel, S.B., Altshuler, D., Daly, M.J., 2011. A framework for variation discovery and genotyping using next-generation DNA sequencing data. Nat. Genet. 43, 491–501. https://doi.org/10.1038/ng.806

Elderfield, H., Ferretti, P., Greaves, M., Crowhurst, S., McCave, I.N., Hodell, D., Piotrowski, A.M., 2012. Evolution of ocean temperature and ice volume through the mid-pleistocene climate transition. Science 337, 704–709. https://doi.org/10.1126/science.1221294

Endler, J.A., 1977. Geographic variation, speciation, and clines. Princeton University Press.

Ewing, G.B., Jensen, J.D., 2016. The consequences of not accounting for background selection in demographic inference. Mol. Ecol. 25, 135–141. https://doi.org/10.1111/mec.13390

Excoffier, L., Dupanloup, I., Huerta-Sánchez, E., Sousa, V.C., Foll, M., 2013. Robust Demographic Inference from Genomic and SNP Data. PLoS Genet. 9. https://doi.org/10.1371/journal.pgen.1003905

Excoffier, L., Marchi, N., Marques, D.A., Matthey-Doret, R., Gouy, A., Sousa, V.C., 2021. Fastsimcoal2: Demographic inference under complex evolutionary scenarios. Bioinformatics 37, 4882–4885. https://doi.org/10.1093/bioinformatics/btab468

Fabry, V., McClintock, J., Mathis, J., Grebmeier, J., 2009. Ocean acidification at high latitudes: The bellwether. Oceanography 22, 160–171. https://doi.org/10.5670/oceanog.2009.105

Faria, R., Johannesson, K., Stankowski, S., 2021. Speciation in marine environments: Diving under the surface. J. Evol. Biol. 34, 4–15. https://doi.org/10.1111/jeb.13756

Felsenstein, J., 2006. Accuracy of coalescent likelihood estimates: Do we need more sites, more sequences, or more loci? Mol. Biol. Evol. 23, 691–700. https://doi.org/10.1093/molbev/msj079

Filatov, D.A., Bendif, E.M., Archontikis, O.A., Hagino, K., Rickaby, R.E.M., 2021. The mode of speciation during a recent radiation in open-ocean phytoplankton. Curr. Biol. 31, 1–11. https://doi.org/10.1016/j.cub.2021.09.073

Fišer, C., Robinson, C.T., Malard, F., 2018. Cryptic species as a window into the paradigm shift of the species concept. Mol. Ecol. 27, 613–635. https://doi.org/10.1111/mec.14486

Accepted Article

1365294x, ja, Downloaded from https://onlinelibrary.wiley.com/doi/10.1111/mec.16931 by Universitaet Bern, Wiley Online Library on [22/03/2023]. See the Terms and Conditions (https://onlinelibrary.wiley.com/terms-and-conditions) on Wiley Online Library for rules of use; OA articles are governed by the applicable Creative Commons License

Accepted Article

Fitzpatrick, B.M., Fordyce, J.A., Gavrilets, S., 2009. Pattern, process and geographic modes of speciation. J. Evol. Biol. 22, 2342–2347. https://doi.org/10.1111/j.1420-9101.2009.01833.x

Fleminger, A., Hulsemann, K., 1987. Geographical variation in *Calanus helgolandicus* s.l. (Copepoda, Calanoida) and evidence of recent speciation of the Black Sea population. Biol. Oceanogr. 5, 43–81. https://doi.org/10.1080/01965581.1987.10749505

Freeman, B.G., Pennell, M.W., 2021. The latitudinal taxonomy gradient. Trends Ecol. Evol. 36, 778–786. https://doi.org/10.1016/j.tree.2021.05.003

Galtier, N., 2016. Adaptive protein evolution in animals and the effective population size hypothesis. PLOS Genet. 12, e1005774. https://doi.org/10.1371/journal.pgen.1005774

Goetze, E., 2005. Global population genetic structure and biogeography of the oceanic copepods *Eucalanus hyalinus* and *E. spinifer*. Evolution 59, 2378–2398. https://doi.org/10.1111/j.0014-3820.2005.tb00948.x

Goetze, E., Andrews, K.R., Peijnenburg, K.T.C.A., Portner, E., Norton, E.L., 2015. Temporal stability of genetic structure in a mesopelagic copepod. PLoS One 10, e0136087. https://doi.org/10.1371/journal.pone.0136087

Goetze, E., Hüdepohl, P.T., Chang, C., Van Woudenberg, L., Iacchei, M., Peijnenburg, K.T.C.A., 2017. Ecological dispersal barrier across the equatorial Atlantic in a migratory planktonic copepod. Prog. Oceanogr. 158, 203–212. https://doi.org/10.1016/j.pocean.2016.07.001

Goetze, E., Kiørboe, T., 2008. Heterospecific mating and species recognition in the planktonic marine copepods Temora stylifera and T. longicornis. Mar. Ecol. Prog. Ser. 375, 185–198. https://doi.org/10.3354/meps07616

Gompel, N., Prud'homme, B., Wittkopp, P.J., Kassner, V.A., Carroll, S.B., 2005. Chance caught on the wing: cis-regulatory evolution and the origin of pigment patterns in *Drosophila*. Nature 433, 481–487.

Groot, C., Margolis, L., 1991. Pacific salmon life histories. UBC Press, Vancouver.

Guerra-Varela, J., Colson, I., Backeljau, T., Breugelmans, K., Hughes, R.N., Rolán-Alvarez, E., 2009. The evolutionary mechanism maintaining shell shape and molecular differentiation between two ecotypes of the dogwhelk *Nucella lapillus*. Evol. Ecol. 23, 261–280. https://doi.org/10.1007/s10682-007-9221-5

Halbert, K.M.K., Goetze, E., Carlon, D.B., 2013. High cryptic diversity across the global range of the migratory planktonic copepods *Pleuromamma piseki* and *P. gracilis*. PLoS One 8, e77011. https://doi.org/10.1371/journal.pone.0077011

Hammer, Ø., Harper, D.A.T., Ryan, P.D., 2001. PAST: Paleontological statistics software package for education and data analysis. Paleontol. Electron. 4, 9.

Hansson, L.A., 2000. Induced pigmentation in zooplankton: A trade-off between threats from predation and ultraviolet radiation. Proc. R. Soc. B Biol. Sci. 267, 2327–2331. https://doi.org/10.1098/rspb.2000.1287

Harvey, B.P., Al-Janabi, B., Broszeit, S., Cioffi, R., Kumar, A., Aranguren-Gassis, M., Bailey, A., Green, L., Gsottbauer, C.M., Hall, E.F., Lechler, M., Mancuso, F.P., Pereira, C.O., Ricevuto, E., Schram, J.B., Stapp, L.S., Stenberg, S., Santa Rosa, L.T., 2014.

1365294x, ja, Downloaded from https://onlinelibrary.wiley.com/doi/10.1111/mec.16931 by Universitaet Bern, Wiley Online Library on [22/03/2023]. See the Terms and Conditions (https://onlinelibrary.wiley.com/terms-and-conditions) on Wiley Online Library for rules of use; OA articles are governed by the applicable Creative Commons License

Accepted Article

Evolution of marine organisms under climate change at different levels of biological organisation. Water (Switzerland) 6, 3545–3574. https://doi.org/10.3390/w6113545

Hirai, J., Tsuda, A., Goetze, E., 2015. Extensive genetic diversity and endemism across the global range of the oceanic copepod *Pleuromamma abdominalis*. Prog. Oceanogr. 138, 77–90. https://doi.org/10.1016/j.pocean.2015.09.002

Hoffman, J.I., Peck, L.S., Hillyard, G., Zieritz, A., Clark, M.S., 2010. No evidence for genetic differentiation between Antarctic limpet *Nacella concinna* morphotypes. Mar. Biol. 157, 765–778. https://doi.org/10.1007/s00227-009-1360-5

Hollander, J., Butlin, R.K., 2010. The adaptive value of phenotypic plasticity in two ecotypes of a marine gastropod. BMC Evol. Biol. 10, 333. https://doi.org/10.1186/1471-2148-10-333

Hollander, J., Collyer, M.L., Adams, D.C., Johannesson, K., 2006. Phenotypic plasticity in two marine snails: Constraints superseding life history. J. Evol. Biol. 19, 1861–1872. https://doi.org/10.1111/j.1420-9101.2006.01171.x

Hönisch, B., Hemming, N.G., 2005. Surface ocean pH response to variations in pCO_2 through two full glacial cycles. Earth Planet. Sci. Lett. 236, 305–314. https://doi.org/10.1016/j.epsl.2005.04.027

Hönisch, B., Ridgwell, A., Schmidt, D.N., Thomas, E., Gibbs, S.J., Sluijs, A., Zeebe, R., Kump, L., Martindale, R.C., Greene, S.E., Kiessling, W., Ries, J., Zachos, J.C., Royer, D.L., Barker, S., Marchitto, T.M., Moyer, R., Pelejero, C., Ziveri, P., Foster, G.L., Williams, B., 2012. The Geological Record of Ocean Acidification. Science 335, 1058–1063. https://doi.org/10.1126/science.1208277

Howard, W.R., 1997. A warm future in the past. Nature 388, 418–419. https://doi.org/10.1038/41201

Hunt, B., Strugnell, J., Bednarsek, N., Linse, K., Nelson, R.J., Pakhomov, E., Seibel, B., Steinke, D., Würzberg, L., 2010. Poles apart: The "bipolar" pteropod species *Limacina helicina* is genetically distinct between the Arctic and Antarctic oceans. PLoS One 5, e9835. https://doi.org/10.1371/journal.pone.0009835

Hunt, B.P.V., Pakhomov, E.A., Hosie, G.W., Siegel, V., Ward, P., Bernard, K., 2008. Pteropods in Southern Ocean ecosystems. Prog. Oceanogr. 78, 193–221. https://doi.org/10.1016/j.pocean.2008.06.001

Janssen, A.W., Peijnenburg, K.T.C.A., 2017. An overview of the fossil record of Pteropoda (Mollusca, Gastropoda, Heterobranchia). Cainozoic Res. 17, 3–10.

Jennings, R.M., Bucklin, A., Ossenbrügger, H., Hopcroft, R.R., 2010. Species diversity of planktonic gastropods (Pteropoda and Heteropoda) from six ocean regions based on DNA barcode analysis. Deep Sea Res. Part II Top. Stud. Oceanogr. 57, 2199–2210. https://doi.org/10.1016/j.dsr2.2010.09.022

Johannesson, K., 2003. Evolution in *Littorina*: Ecology matters. J. Sea Res. 49, 107–117. https://doi.org/10.1016/S1385-1101(02)00218-6

Johannesson, K., Panova, M., Kemppainen, P., André, C., Rolan-Alvarez, E., Butlin, R.K., 2010. Repeated evolution of reproductive isolation in a marine snail: Unveiling mechanisms of speciation. Philos. Trans. R. Soc. B Biol. Sci. 365, 1735–1747. https://doi.org/10.1098/rstb.2009.0256

1365294x, ja, Downloaded from https://onlinelibrary.wiley.com/doi/10.1111/mec.16931 by Universitaet Bern, Wiley Online Library on [22/03/2023]. See the Terms and Conditions (https://onlinelibrary.wiley.com/terms-and-conditions) on Wiley Online Library for rules of use; OA articles are governed by the applicable Creative Commons License

Accepted Article

Johnsen, S., 2001. Hidden in plain sight: The ecology and physiology of organismal transparency. Biol. Bull. 201, 301–318. https://doi.org/10.2307/1543609

Karakas, F., Wingate, J., Blanco-Bercial, L., Maas, A.E., Murphy, D.W., 2020. Swimming and sinking behavior of warm water pelagic snails. Front. Mar. Sci. 7, 749. https://doi.org/10.3389/fmars.2020.556239

Kass, R.E., Raftery, A.E., 1995. Bayes factors. J. Am. Stat. Assoc. 90, 773–795. https://doi.org/10.1080/01621459.1995.10476572

Katoh, K., Standley, D.M., 2013. MAFFT multiple sequence alignment software version 7: Improvements in performance and usability. Mol. Biol. Evol. 30, 772–780. https://doi.org/10.1093/molbev/mst010

Kender, S., McClymont, E.L., Elmore, A.C., Emanuele, D., Leng, M.J., Elderfield, H., 2016. Mid Pleistocene foraminiferal mass extinction coupled with phytoplankton evolution. Nat. Commun. 7, 11970. https://doi.org/10.1038/ncomms11970

Kiørboe, T., 2007. Mate finding, mating, and population dynamics in a planktonic copepod *Oithona davisae*: There are too few males. Limnol. Oceanogr. 52, 1511–1522. https://doi.org/10.4319/lo.2007.52.4.1511

Knowlton, N., 1993. Sibling species in the sea. Annu. Rev. Ecol. Syst. 24, 189–216. https://doi.org/10.1146/annurev.es.24.110193.001201

Krug, P.J., Vendetti, J.E., Rodriguez, A.K., Retana, J.N., Hirano, Y.M., Trowbridge, C.D., 2013. Integrative species delimitation in photosynthetic sea slugs reveals twenty candidate species in three nominal taxa studied for drug discovery, plastid symbiosis or biological control. Mol. Phylogenet. Evol. 69, 1101–1119. https://doi.org/10.1016/j.ympev.2013.07.009

Kucera, M., Darling, K.F., 2002. Cryptic species of planktonic foraminifera: Their effect on palaeoceanographic reconstructions. Philos. Trans. R. Soc. A Math. Phys. Eng. Sci. 360, 695–718. https://doi.org/10.1098/rsta.2001.0962

Laibl, C.F., Schrödl, M., Kohnert, P.C., 2019. 3D-microanatomy of a keystone planktonic species, the northern polar pteropod *Limacina helicina helicina* (Gastropoda: Heterobranchia). J. Molluscan Stud. 85, 133–142. https://doi.org/10.1093/mollus/eyy063

Lalli, C.M., Gilmer, R.W., 1989. Pelagic snails: The biology of holoplanktonic gastropod molluscs. Stanford University Press, California.

Lalli, C.M., Wells, F.E., 1978. Reproduction in the genus *Limacina* (Ophistobranchia: Thecosomata). J. Zool. 186, 95–108.

Lambeck, K., Chappell, J., 2001. Sea level change through the last glacial cycle. Science 292, 679–686. https://doi.org/10.1126/science.1059549

Leaché, A.D., Fujita, M.K., Minin, V.N., Bouckaert, R.R., 2014. Species delimitation using genome-wide SNP Data. Syst. Biol. 63, 534–542. https://doi.org/10.1093/sysbio/syu018

Lefébure, T., Douady, C.J., Gouy, M., Gibert, J., 2006. Relationship between morphological taxonomy and molecular divergence within Crustacea: Proposal of a molecular threshold to help species delimitation. Mol. Phylogenet. Evol. 40, 435–447. https://doi.org/10.1016/j.ympev.2006.03.014

1365294x, ja, Downloaded from https://onlinelibrary.wiley.com/doi/10.1111/mec.16931 by Universitaet Bern, Wiley Online Library on [22/03/2023]. See the Terms and Conditions (https://onlinelibrary.wiley.com/terms-and-conditions) on Wiley Online Library for rules of use; OA articles are governed by the applicable Creative Commons License

Accepted Article

Leffler, E.M., Bullaughey, K., Matute, D.R., Meyer, W.K., Ségurel, L., Venkat, A., Andolfatto, P., Przeworski, M., 2012. Revisiting an Old Riddle: What Determines Genetic Diversity Levels within Species? PLoS Biol. 10, e1001388. https://doi.org/10.1371/journal.pbio.1001388

Leigh, J.W., Bryant, D., 2015. POPART: Full-feature software for haplotype network construction. Methods Ecol. Evol. 6, 1110–1116. https://doi.org/10.1111/2041-210X.12410

Li, H., 2013. Aligning sequence reads, clone sequences and assembly contigs with BWA-MEM. arxiv Prepr. 00, 1–3.

Li, H., Handsaker, B., Wysoker, A., Fennell, T., Ruan, J., Homer, N., Marth, G., Abecasis, G., Durbin, R., 2009. The sequence Alignment/Map format and SAMtools. Bioinformatics 25, 2078–2079. https://doi.org/10.1093/bioinformatics/btp352

Lisiecki, L.E., Raymo, M.E., 2005. A Pliocene-Pleistocene stack of 57 globally distributed benthic $\delta^{18}O$ records. Paleoceanography 20, PA1003. https://doi.org/10.1029/2004PA001071

Liu, X., Fu, Y.-X., 2020. Stairway Plot 2: demographic history inference with folded SNP frequency spectra. Genome Biol. 21, 280. https://doi.org/10.1186/s13059-020-02196-9

Malinsky, M., Matschiner, M., 2021. Dsuite - Fast D -statistics and related admixture evidence from VCF files 584–595. https://doi.org/10.1111/1755-0998.13265

Malinsky, M., Trucchi, E., Lawson, D.J., Falush, D., 2018. RADpainter and fineRADstructure: Population inference from RADseq data. Mol. Biol. Evol. 35, 1284–1290. https://doi.org/10.1093/molbev/msy023

Mani, G.S., Clarke, B.C., 1990. Mutational order: A major stochastic process in evolution. Proc. R. Soc. B Biol. Sci. 240, 29–37. https://doi.org/10.1098/rspb.1990.0025

Manno, C., Bednaršek, N., Tarling, G.A., Peck, V.L., Comeau, S., Adhikari, D., Bakker, D.C.E., Bauerfeind, E., Bergan, A.J., Berning, M.I., Buitenhuis, E., Burridge, A.K., Chierici, M., Flöter, S., Fransson, A., Gardner, J., Howes, E.L., Keul, N., Kimoto, K., Kohnert, P., Lawson, G.L., Lischka, S., Maas, A., Mekkes, L., Oakes, R.L., Pebody, C., Peijnenburg, K.T.C.A., Seifert, M., Skinner, J., Thibodeau, P.S., Wall-Palmer, D., Ziveri, P., 2017. Shelled pteropods in peril: Assessing vulnerability in a high CO_2 ocean. Earth-Science Rev. 169, 132–145. https://doi.org/10.1016/j.earscirev.2017.04.005

Manno, C., Rumolo, P., Barra, M., D'Albero, S., Basilone, G., Genovese, S., Mazzola, S., Bonanno, A., 2018. Condition of pteropod shells near a volcanic CO_2 vent region. Mar. Environ. Res. 143, 39–48. https://doi.org/10.1016/j.marenvres.2018.11.003

Manno, C., Tirelli, V., Accornero, A., Fonda Umani, S., 2010. Importance of the contribution of *Limacina helicina* faecal pellets to the carbon pump in Terra Nova Bay (Antarctica). J. Plankton Res. 32, 145–152. https://doi.org/10.1093/plankt/fbp108

Mariani, S., Peijnenburg, K.T.C.A., Weetman, D., 2012. Independence of neutral and adaptive divergence in a low dispersal marine mollusc. Mar. Ecol. Prog. Ser. 446, 173–187. https://doi.org/10.3354/meps09507

Mayr, E., 1954. Geographic speciation in tropical echnoids. Evolution 8, 1–18. https://doi.org/https://doi.org/10.1111/j.1558-5646.1954.tb001 04.x

1365294x, ja, Downloaded from https://onlinelibrary.wiley.com/doi/10.1111/mec.16931 by Universitaet Bern, Wiley Online Library on [22/03/2023]. See the Terms and Conditions (https://onlinelibrary.wiley.com/terms-and-conditions) on Wiley Online Library for rules of use; OA articles are governed by the applicable Creative Commons License

McClymont, E.L., Sosdian, S.M., Rosell-Melé, A., Rosenthal, Y., 2013. Pleistocene sea-surface temperature evolution: Early cooling, delayed glacial intensification, and implications for the mid-Pleistocene climate transition. Earth-Science Rev. 123, 173–193. https://doi.org/10.1016/j.earscirev.2013.04.006

McManus, G.B., Katz, L.A., 2009. Molecular and morphological methods for identifying plankton: what makes a successful marriage? J. Plankton Res. 31, 1119–1129. https://doi.org/10.1093/plankt/fbp061

McManus, J., Oppo, D., Cullen, J., Healey, S., 2003. Marine isotope stage 11 (MIS 11): Analog for holocene and future climate? Geophys. Monogr. Ser. 137, 69–85. https://doi.org/10.1029/137GM06

Mekkes, L., Renema, W., Bednaršek, N., Alin, S.R., Feely, R.A., Huisman, J., Roessingh, P., Peijnenburg, K.T.C.A., 2021a. Pteropods make thinner shells in the upwelling region of the California Current Ecosystem. Sci. Rep. 11, 1731. https://doi.org/10.1038/s41598-021-81131-9

Mekkes, L., Sepúlveda-Rodríguez, G., Bielkinaitė, G., Wall-Palmer, D., Brummer, G.-J.A., Dämmer, L.K., Huisman, J., van Loon, E., Renema, W., Peijnenburg, K.T.C.A., 2021b. Effects of ocean acidification on calcification of the sub-Antarctic pteropod Limacina retroversa. Front. Mar. Sci. 8, 581432. https://doi.org/10.3389/fmars.2021.581432

Milá, B., Van Tassell, J.L., Calderón, J.A., Rüber, L., Zardoya, R., 2017. Cryptic lineage divergence in marine environments: genetic differentiation at multiple spatial and temporal scales in the widespread intertidal goby *Gobiosoma bosc*. Ecol. Evol. 7, 5514–5523. https://doi.org/10.1002/ece3.3161

Monnin, E., Indermuhle, A., Dallenbach, A., Fluckiger, J., Stauffer, B., Stocker, T.F., Raynaud, D., Barnolaz, J., 2001. Atmospheric CO_2 Concentrations over the Last Glacial Termination. Science 291, 112–114.

Munday, P.L., Warner, R.R., Monro, K., Pandolfi, J.M., Marshall, D.J., 2013. Predicting evolutionary responses to climate change in the sea. Ecol. Lett. 16, 1488–1500. https://doi.org/10.1111/ele.12185

Nichols, R., 2001. Gene trees and species trees are not the same. Sci. Direct 16, 358–364.

Niemi, A., Bednaršek, N., Michel, C., Feely, R.A., Williams, W., Azetsu-Scott, K., Walkusz, W., Reist, J.D., 2021. Biological impact of ocean acidification in the Canadian Arctic: Widespread severe pteropod shell dissolution in Amundsen Gulf. Front. Mar. Sci. 8, 600184. https://doi.org/10.3389/fmars.2021.600184

Norris, R.D., 2000. Pelagic species diversity, biogeography, and evolution. Paleobiology 26, 236–258. https://doi.org/doi:10.1017/s0094837300026956

Oksanen, J., Guillaume Blanchet, F., Friendly, M., Kindt, R., Legendre, P., McGlinn, D., Minchin, P.R., O'Hara, R.B., Simpson, G.L., Solymos, P., Stevens, M.H.H., Szoecs, E., Wagner, H., 2019. vegan: Community Ecology Package.

Padial, J.M., Miralles, A., De la Riva, I., Vences, M., 2010. The integrative future of taxonomy. Front. Zool. 7, 16. https://doi.org/10.1186/1742-9994-7-16

Palumbi, S.R., 1994. Genetic divergence, reproductive isolation, and marine speciation. Annu. Rev. Ecol. Syst. 25, 547–572.

Accepted Article

1365294x, ja, Downloaded from https://onlinelibrary.wiley.com/doi/10.1111/mec.16931 by Universitaet Bern, Wiley Online Library on [22/03/2023]. See the Terms and Conditions (https://onlinelibrary.wiley.com/terms-and-conditions) on Wiley Online Library for rules of use; OA articles are governed by the applicable Creative Commons License

Accepted Article

Peijnenburg, K.T.C.A., Goetze, E., 2013. High evolutionary potential of marine zooplankton. Ecol. Evol. 3, 2765–2783. https://doi.org/10.1002/ece3.644

Peijnenburg, K.T.C.A., Janssen, A.W., Wall-Palmer, D., Goetze, E., Maas, A.E., Todd, J.A., Marlétaz, F., 2020. The origin and diversification of pteropods precede past perturbations in the Earth's carbon cycle. Proc. Natl. Acad. Sci. 117, 25609–25617. https://doi.org/10.1073/pnas.1920918117

Petrick, B., Martínez-García, A., Auer, G., Reuning, L., Auderset, A., Deik, H., Takayanagi, H., De Vleeschouwer, D., Iryu, Y., Haug, G.H., 2019. Glacial Indonesian Throughflow weakening across the Mid-Pleistocene Climatic Transition. Sci. Rep. 9, 16995. https://doi.org/10.1038/s41598-019-53382-0

Poloczanska, E.S., Burrows, M.T., Brown, C.J., García Molinos, J., Halpern, B.S., Hoegh-Guldberg, O., Kappel, C. V., Moore, P.J., Richardson, A.J., Schoeman, D.S., Sydeman, W.J., 2016. Responses of marine organisms to climate change across oceans. Front. Mar. Sci. 3, 62. https://doi.org/10.3389/fmars.2016.00062

Potkamp, G., Fransen, C.H.J.M., 2019. Speciation with gene flow in marine systems. Contrib. to Zool. 88, 133–172. https://doi.org/10.1163/18759866-20191344

R Core Team, 2017. R: A language and environment for statistical computing.

Rambaut, A., Drummond, A.J., Xie, D., Baele, G., Suchard, M.A., 2018. Posterior summarization in Bayesian phylogenetics using Tracer 1.7. Syst. Biol. 67, 901–904. https://doi.org/10.1093/sysbio/syy032

Rohlf, F.J., 2015. The tps series of software. Hystrix 26, 9–12. https://doi.org/10.4404/hystrix-26.1-11264

Rohlf, F.J., Slice, D., 1990. Extension of the procrustes method for the optimal superimposition of landmarks. Syst. Zool 39, 40–59.

Rolán, E., Guerra-Varela, J., Colson, I., Hughes, R.N., Rolán-Alvarez, E., 2004. Morphological and genetic analysis of two sympatric morphs of the dogwhelk *Nucella lapillus* (Gastropoda: Muricidae) from Galicia (Northwestern Spain). J. Molluscan Stud. 70, 179–185. https://doi.org/10.1093/mollus/70.2.179

Romiguier, J., Gayral, P., Ballenghien, M., Bernard, A., Cahais, V., Chenuil, A., Chiari, Y., Dernat, R., Duret, L., Faivre, N., Loire, E., Lourenco, J.M., Nabholz, B., Roux, C., Tsagkogeorga, G., Weber, A.A.T., Weinert, L.A., Belkhir, K., Bierne, N., Glémin, S., Galtier, N., 2014. Comparative population genomics in animals uncovers the determinants of genetic diversity. Nature 515, 261–263. https://doi.org/10.1038/nature13685

Sáez, A.G., Probert, I., Geisen, M., Quinn, P., Young, J.R., Medlin, L.K., 2003. Pseudo-cryptic speciation in coccolithophores. Proc. Natl. Acad. Sci. U. S. A. 100, 7163–7168. https://doi.org/10.1073/pnas.1132069100

Sanyal, A., Hemming, N.G., Hanson, G.N., Broecker, W.S., 1995. Evidence for a higher pH in the glacial ocean from boron isotopes in foraminifera. Nature 373, 234–236.

Schluter, D., 2009. Evidence for ecological speciation and its alternative. Science 323, 737–741. https://doi.org/10.1126/science.1160006

Schluter, D., Conte, G.L., 2009. Genetics and ecological speciation. Light Evol. 3, 47–64.

1365294x, ja, Downloaded from https://onlinelibrary.wiley.com/doi/10.1111/mec.16931 by Universitaet Bern, Wiley Online Library on [22/03/2023]. See the Terms and Conditions (https://onlinelibrary.wiley.com/terms-and-conditions) on Wiley Online Library for rules of use; OA articles are governed by the applicable Creative Commons License

Accepted Article

https://doi.org/10.17226/12692

Shimizu, K., Noshita, K., Kimoto, K., Sasaki, T., 2021. Phylogeography and shell morphology of the pelagic snail *Limacina helicina* in the Okhotsk Sea and western North Pacific. Mar. Biodivers. 51, 22. https://doi.org/10.1007/s12526-021-01166-z

Siegenthaler, U., Stocker, T.F., Monnin, E., Lüthi, D., Schwander, J., Stauffer, B., Raynaud, D., Barnola, J.-M., Fischer, H., Masson-Delmotte, V., Jouzel, J., 2005. Stable Carbon Cycle–Climate Relationship During the Late Pleistocene. Science 310, 1313–1317. https://doi.org/10.1126/science.1120130

Stange, M., Sánchez-Villagra, M.R., Salzburger, W., Matschiner, M., 2018. Bayesian divergence-time estimation with genome-wide single-nucleotide polymorphism data of sea catfishes (Ariidae) supports Miocene closure of the Panamanian Isthmus. Syst. Biol. 67, 681–699. https://doi.org/10.1093/sysbio/syy006

Sulpis, O., Jeansson, E., Dinauer, A., Lauvset, S.K., Middelburg, J.J., 2021. Calcium carbonate dissolution patterns in the ocean. Nat. Geosci. 14, 423–428. https://doi.org/10.1038/s41561-021-00743-y

Sunday, J.M., Calosi, P., Dupont, S., Munday, P.L., Stillman, J.H., Reusch, T.B.H., 2014. Evolution in an acidifying ocean. Trends Ecol. Evol. 29, 117–125. https://doi.org/10.1016/j.tree.2013.11.001

Tange, O., 2011. GNU Parallel: The command-line power tool. ;login USENIX Mag. https://doi.org/http://dx.doi.org/10.5281/zenodo.16303

Telesca, L., Michalek, K., Sanders, T., Peck, L.S., Thyrring, J., Harper, E.M., 2018. Blue mussel shell shape plasticity and natural environments: a quantitative approach. Sci. Rep. 8, 2865. https://doi.org/10.1038/s41598-018-20122-9

van der Spoel, S., Heyman, R.P., 1983. A comparative atlas of zooplankton: Biological patterns in the oceans. Wetenschappelijke uitgeverij Bunge, Utrecht.

van der Spoel, S., Newman, L.J., Estep, K.W., 1997. Pelagic molluscs of the world. ETI World Biodivers. Database CD-ROM Ser.

Wall-Palmer, D., Burridge, A.K., Goetze, E., Stokvis, F.R., Janssen, A.W., Mekkes, L., Moreno-Alcántara, M., Bednaršek, N., Schiøtte, T., Sørensen, M.V., Smart, C.W., Peijnenburg, K.T.C.A., 2018. Biogeography and genetic diversity of the atlantid heteropods. Prog. Oceanogr. 160, 1–25. https://doi.org/10.1016/j.pocean.2017.11.004

Wall-Palmer, D., Smart, C.W., Hart, M.B., Leng, M.J., Conversi, A., Borghini, M., Manini, E., Aliani, S., 2014. Late Pleistocene pteropods, heteropods and planktonic foraminifera from the Caribbean Sea, Mediterranean Sea and Indian Ocean. Micropaleontology 60, 557–578.

Weiner, A.K.M., Weinkauf, M.F.G., Kurasawa, A., Darling, K.F., Kucera, M., Grimm, G.W., 2014. Phylogeography of the tropical planktonic foraminifera lineage *Globigerinella* reveals isolation inconsistent with passive dispersal by ocean currents. PLoS One 9, e92148. https://doi.org/10.1371/journal.pone.0092148

Weir, B.S., Cockerham, C.C., 1984. Estimating F-Statistics for the Analysis of Population Structure Author (s): B . S . Weir and C . Clark Cockerham Published by: Society for the Study of Evolution Stable URL: http://www.jstor.org/stable/2408641. Evolution 38, 1358–1370.

1365294x, ja, Downloaded from https://onlinelibrary.wiley.com/doi/10.1111/mec.16931 by Universitaet Bern, Wiley Online Library on [22/03/2023]. See the Terms and Conditions (https://onlinelibrary.wiley.com/terms-and-conditions) on Wiley Online Library for rules of use; OA articles are governed by the applicable Creative Commons License

Wells, F.E., 1976. Growth rate of four species of euthecosomatous pteropods occuring off Barbados, West Indies. The Natutilus 90, 114–116.

Whittaker, K.A., Rynearson, T.A., 2017. Evidence for environmental and ecological selection in a microbe with no geographic limits to gene flow. Proc. Natl. Acad. Sci. U. S. A. 114, 2651–2656. https://doi.org/10.1073/pnas.1612346114

Wiernasz, D.C., Kingsolver, J.G., 1992. Wing melanin pattern mediates species recognition in *Pieris occidentalis*. Anim. Behav. 43, 89–94. https://doi.org/10.1016/S0003-3472(05)80074-0

Williams, S.T., 2017. Molluscan shell colour. Biol. Rev. 92, 1039–1058. https://doi.org/10.1111/brv.12268

Wormuth, J.H., 1981. Vertical distributions and diel migrations of Euthecosomata in the northwest Sargasso Sea. Deep Sea Res. Part A, Oceanogr. Res. Pap. 28, 1493–1515. https://doi.org/10.1016/0198-0149(81)90094-7

Young, R.G., Abbott, C.L., Therriault, T.W., Adamowicz, S.J., Hogg, I., 2017. Barcode-based species delimitation in the marine realm: A test using Hexanauplia (Multicrustacea: Thecostraca and Copepoda). Genome 60, 169–182. https://doi.org/10.1139/gen-2015-0209

Zeebe, R.E., Ridgwell, A., Zachos, J.C., 2016. Anthropogenic carbon release rate unprecedented during the past 66 million years. Nat. Geosci. 9, 325–329. https://doi.org/10.1038/ngeo2681

Zelditch, M.L., Swiderski, D.L., Sheets, H.D., Fink, W.L., 2004. Geometric morphometrics for biologists: A primer. Elsevier Academic Press, San Diego and London.

Zieritz, A., Hoffman, J.I., Amos, W., Aldridge, D.C., 2010. Phenotypic plasticity and genetic isolation-by-distance in the freshwater mussel *Unio pictorum* (Mollusca: Unionoida). Evol. Ecol. 24, 923–938. https://doi.org/10.1007/s10682-009-9350-0

Accepted Article

1365294x, ja, Downloaded from https://onlinelibrary.wiley.com/doi/10.1111/mec.16931 by Universitaet Bern, Wiley Online Library on [22/03/2023]. See the Terms and Conditions (https://onlinelibrary.wiley.com/terms-and-conditions) on Wiley Online Library for rules of use; OA articles are governed by the applicable Creative Commons License